

## UNITARY A-CURRENTS OF RAT LOCUS COERULEUS NEURONES GROWN IN CELL CULTURE: RECTIFICATION CAUSED BY INTERNAL $\text{Mg}^{2+}$ AND $\text{Na}^+$

By I. D. FORSYTHE, P. LINSDELL AND P. R. STANFIELD

*From the Department of Physiology, University of Leicester, PO Box 138,  
Leicester LE1 9HN*

*(Received 4 September 1991)*

### SUMMARY

1. We have used whole-cell and single-channel recording to study the transient outward potassium current (A-current) of rat locus coeruleus neurones grown in tissue culture. The A-current was largely inactivated at the resting potential, but could be activated from sufficiently negative holding potentials during steps positive to  $-50$  mV. The current was sensitive to 4-aminopyridine. Another slowly activating, sustained current was similar to a delayed rectifier.

2. In the on-cell configuration the unitary conductance of channels carrying A-current was  $40.9 \pm 2.2$  pS ( $n = 6$ ) with high external potassium (140 mM) and  $14.8 \pm 1.4$  pS ( $n = 11$ ) with 3 mM  $[\text{K}^+]_o$ . The unitary current–voltage relation was not linear, but had a negative slope at very positive voltages in 3 mM  $[\text{K}^+]_o$ . The reversal potential changed with  $[\text{K}^+]_o$  as expected for a  $\text{K}^+$  channel.

3. The open state probability of A-current channels was voltage dependent, reaching a peak of  $0.78 \pm 0.17$  (seven patches). The relationships between both activation and inactivation and membrane potential were well fitted by Boltzmann expressions. Activation was half-maximum at a potential  $71.9 \pm 11.8$  mV ( $n = 4$ ) positive to the resting potential (approximately  $-61$  mV). Inactivation was half-complete  $29.4 \pm 3.8$  mV ( $n = 4$ ) negative to the resting potential. There was evidence from runs analysis for slow inactivation of channels.

4. Channels showed frequent visits to substates, the most readily identifiable of which had an amplitude  $0.55 \pm 0.04$  ( $n = 5$ ) of the fully open state. Other substates had amplitudes of around 0.25 and 0.75. Occupancy of substates was greater at negative membrane potentials.

5. A preliminary analysis of kinetic behaviour, treating visits to substates as openings, shows that open times are distributed as a single exponential. The open time was 16.2 ms ( $n = 4$ ) at a voltage 100 mV positive to the resting potential, increasing with further depolarization. Closed times are distributed as the sum of three or four exponentials. First latency distributions are strongly voltage dependent and show a delay, giving a sigmoidal rise to the distribution. Increasing temperature increased unitary current and reduced mean open time.

6. The mechanism of the rectification seen in the unitary current–voltage relationship was examined using excised, inside-out patches. When 140 mM-KCl

solutions containing no divalent cations and no  $\text{Na}^+$  were applied to the intracellular face of such a patch, the relation between unitary A-currents and voltage became linear (slope conductance  $17.8 \pm 1.8$  pS,  $n = 16$ , when  $[\text{K}^+]_o = 3$  mM). Addition of  $\text{Mg}^{2+}$  (2–10 mM) or  $\text{Na}^+$  (10–20 mM) to the internal surface was found to reduce outward currents, inducing rectification similar to that seen during on-cell recording.

7. Analysis of the block by intracellular  $\text{Mg}^{2+}$  and  $\text{Na}^+$  gave estimates for the dissociation constant for  $\text{Mg}^{2+}$  of  $15.5 \pm 1.5$  mM ( $n = 6$ ) at zero voltage, while that for  $\text{Na}^+$  was  $76.0 \pm 7.2$  mM ( $n = 3$ ). The Hill coefficient was close to 1 in each case. The voltage dependence of the block suggests an apparent valency of 0.51 for  $\text{Mg}^{2+}$  and 0.78 for  $\text{Na}^+$ .

8. The open time was unaffected by excision of the patch from an on-cell to the inside-out configuration. Perfusion of an excised inside-out patch with  $\text{Mg}^{2+}$  reduced current without affecting open time, implying that the blocking ion can unbind from the closed channel.

9. Preliminary analysis of the open and closed times is consistent with a kinetic scheme with four closed, one open and two inactivated states. There must be at least two voltage-dependent transitions between states.

10. The results with intracellular blocking ions demonstrate that neuronal A-currents, like the inward rectifiers and ATP-dependent  $\text{K}^+$  channels, are modulated by internal  $\text{Mg}^{2+}$  and  $\text{Na}^+$ . Physiologically, this phenomenon will limit the contribution of A-current to repolarization during the overshoot of the action potential. Pathologically, build up of  $[\text{Na}^+]_i$  during excitotoxic phenomena by reducing the effectiveness of this current may contribute to feed-forward excitation.

## INTRODUCTION

A transient outward  $\text{K}^+$  current was first observed by Hagiwara, Kusano & Saito (1961) in molluscan neurones and was subsequently characterized by Connor & Stevens (1971*a, b*) in neurones of a marine gastropod, where it was named  $I_A$ . A-current exhibits rapid activation on depolarization followed by inactivation, giving the current its transient nature. In the steady state, A-current is largely inactivated at the resting potential, so that its activation is dependent on prior hyperpolarization. Similar transient outward  $\text{K}^+$  currents have been identified in many excitable cells including the mammalian peripheral and central nervous system (Galvan, 1982; Gustafsson, Galvan, Grafe & Wigstrom, 1982; Segal, Rogawski & Barker, 1984). Transient outward currents may be distinguished pharmacologically by their sensitivity to 4-aminopyridine (4-AP; Thompson, 1977; Segal *et al.* 1984) and dendrotoxins (Stansfeld, Marsh, Halliwell & Brown, 1986) but they are relatively insensitive to tetraethylammonium (Thompson, 1977). Together these properties permit a reliable distinction to be drawn between A-current and other outward potassium currents, such as the delayed rectifier. Functionally, A-current may contribute to repolarization of the action potential, but a major role may be to regulate action potential frequency (Connor & Stevens, 1971*b*) so influencing information flow in the nervous system.

Recent molecular, pharmacological and electrophysiological studies suggest that there are multiple types of A-current channels. A number of different potassium channel proteins are expressed from the Shaker gene of *Drosophila* by alternative

splicing of the primary mRNA transcript (Schwarz, Tempel, Papazian, Jan & Jan, 1988), and these proteins form A-current channels that inactivate at different rates when expressed in *Xenopus* oocytes (Timpe, Schwarz, Tempel, Papazian, Jan & Jan, 1988). Several different potassium channel genes exist in the rat genome (Stühmer, Ruppersberg, Schröter, Sakmann, Stocker, Giese, Perschke, Baumann & Pongs, 1989; Frech, Van Dongen, Schuster, Brown & Joho, 1989), and the suggestion that transient outward currents in the rat nervous system are heterogeneous from differential sensitivity to 4-AP and dendrotoxin (Stansfeld *et al.* 1986) may be a reflection of differential expression of these genes in different parts of the brain (Beckh & Pongs, 1990).

We have set out to examine A-currents in neurones of the rat locus coeruleus, a brain stem nucleus involved in arousal and attention and known to provide an extensive noradrenergic projection to both cortical and subcortical structures. We have recorded the currents in both on-cell and inside-out patch clamp configurations. The channels have properties broadly similar to those reported in the peripheral nervous system (Cooper & Shrier, 1985, 1989; Kasai, Kameyama, Yamaguchi & Fukuda, 1986). We show that A-channels have a single voltage-dependent open state with three subconductance levels. There are at least three or four closed states. The unitary conductance rectifies at positive potentials, owing to a fast block by internal  $Mg^{2+}$  and  $Na^{+}$ . Preliminary reports of parts of this work have been given elsewhere (Forsythe & Stanfield, 1989; Linsdell, Forsythe & Stanfield, 1990; Forsythe, Linsdell & Stanfield, 1990).

## METHODS

### *Tissue culture*

Primary cell cultures were prepared from Lister hooded rat pups, aged 1–5 days, killed by decapitation. Low-density cultures of neurones from the locus coeruleus were plated onto an astroglial feeder layer, using methods similar to those described previously for locus coeruleus (Masuko, Nakajima, Nakajima & Yamaguchi, 1986) and for hippocampal neurones (Forsythe & Westbrook, 1988). In brief, hippocampal astroglial cells were obtained by plating dissociated hippocampal cells at a density of 62 500 cells per 13 mm glass coverslip, the coverslip having been coated with collagen and poly-L-lysine. The cells were fed at 2 day intervals with a minimal essential medium (MEM, GIBCO 072/01700A) containing 10% fetal calf serum (Advanced Protein Products) until they became confluent (after 10–14 days). Neurones were destroyed by this treatment. Mitosis was then blocked with 5-fluoro-2'-deoxyuridine and uridine and the medium was changed to a feeding medium composed of MEM with 10% heat inactivated horse serum (Advanced Protein Products) at least 24 h before neurones were added. Locus coeruleus neurones were obtained by subjecting the dissected nuclei to digestion with 0.25% trypsin (GIBCO 043/05090H), followed by trituration. The dissociation was conducted in serum-free MEM with an N2 serum supplement (Bottenstein & Sato, 1979) and the cell suspension was added to the confluent feeder-layer using the cells from a single locus coeruleus for each coverslip. Cultures were maintained for up to 6 months by removing half the medium from each well and adding 0.5 ml fresh medium at weekly intervals.

Immunocytochemical studies showed that > 90% of the feeder layer cells contained glial fibrillary acidic protein (GFAP), while > 80% of neurones contained dopamine beta-hydroxylase and tyrosine hydroxylase and showed catecholamine histofluorescence (A. Alibhai & I. D. Forsythe, unpublished observations).

### *Electrophysiology*

An Axopatch 1B amplifier was used for whole-cell and single channel recording. The whole-cell recording pipettes were constructed from thin-walled Pyrex glass and had resistances of 5–8 M $\Omega$  when filled with recording solutions. Recordings of unitary currents were made using electrodes

pulled from thick-walled Pyrex glass, coated with Sylgard to within 200  $\mu\text{m}$  of the tip. The patch pipette solutions are given in Table 1; they contained either 3 or 140 mM-K<sup>+</sup>. Ion channels were judged to be A-type on the basis of their transient activation under depolarization, checked in each patch by ensemble-averaging unitary current records, and their inactivation at holding potentials positive to -60 mV.

TABLE 1. Experimental solutions

Solution	NaCl	KCl	K gluconate	Glucose	HEPES	MgCl <sub>2</sub>	CaCl <sub>2</sub>	EGTA
<b>Extracellular solutions</b>								
ACSF	135	3	—	10	10	1	1	—
3K <sup>+</sup>	135	3	—	10	10	1	2	—
140K <sup>+</sup>	—	140	—	—	10	1	2	—
<b>Intracellular solutions</b>								
WCR	—	—	145	—	10	2	1	11
AICF	—	140	—	—	5	—	—	5

All concentrations in mM. Osmolarity was adjusted with sucrose to 320 mosm for extracellular solutions and 310 mosm for intracellular solutions. The pH of all solutions was adjusted to 7.3. All extracellular solutions contained tetrodotoxin (TTX) at 1  $\mu\text{M}$ .

Data were digitized using a Cambridge Electronic Design (CED) 1401 interface and written to disc for analysis on a Hewlett Packard Vectra E5/12 or Dell 325D computer running CED 'PATCH' software. Step and ramp voltage protocols were also generated using this software. Unless otherwise stated, data were filtered at 2 kHz (-3 dB) using an 8-pole Bessel filter and digitized at 5 or 10 kHz. Outward membrane currents are ascribed a positive sign and shown as upward deflections.

Open and closed times were measured by setting a cursor between open and closed current levels, at approximately 30% of the full open level, and logging events as the current crossed this level. Such a procedure was used, rather than that of setting the cursor midway between open and closed, because of the presence of a prominent substate whose amplitude was around 50% of fully open (see *Results*). Each transition was logged after visual inspection and an idealized record was formed which could be checked against the experimental records. Visits to substates were logged as openings. A minimum resolution was not imposed in this instance. Nor are the open times corrected for missed closures except where indicated in the text.

Histograms of open and closed times were fitted by exponentials or the sum of exponentials using the Simplex least squares fitting routines of the CED software.

#### *Drug application and perfusion*

Experiments were conducted in a Peltier controlled environmental chamber (PDMI-2, Medical Systems Corp.; Forsythe, 1991), which permitted continuous perfusion with artificial cerebrospinal fluid (ACSF) at a controlled temperature. The volume of the experimental chamber was 300–500  $\mu\text{l}$ . In the whole-cell and on-cell patch clamp experiments, ACSF was continually perfused at a rate of 100  $\mu\text{l min}^{-1}$  using a peristaltic pump (Gilson Minipuls 3). The temperature was controlled at 20 °C except where otherwise indicated. 4-Aminopyridine (4-AP) was applied by pressure ejection using a General Valve Picospritzer II from an unpolished patch pipette (puffer pipette) positioned in the vicinity of the soma. During inside-out patch clamp experiments, the gigohm seal was made during perfusion with ACSF, so that the presence of A-channels in the patch could be confirmed in the on-cell configuration before patch excision. The tip of the pipette was then moved so that the exposed cytoplasmic surface of the membrane patch could be shunted between one of three perfusion pipes through which an artificial intracellular fluid (AICF) was pumped. One pipe contained control medium (Table 1) while the others contained the same medium with added Mg<sup>2+</sup> and/or Na<sup>+</sup>.

#### *Experimental results*

Except where otherwise indicated, results are given as mean  $\pm$  standard deviation.

## RESULTS

*Whole-cell recording experiments**Whole-cell A-currents*

Whole-cell patch clamp recordings were made with patch pipettes containing 140 mM-potassium gluconate (WCR solution, Table 1). Figure 1 shows that locus coeruleus neurones in tissue culture express a transient and a sustained outward current. Neurones were voltage clamped at holding potentials of  $-100$  and  $-40$  mV and the membrane potential was subsequently stepped over the range  $-120$  to  $+20$  mV. Leakage currents and capacitive transients were subtracted digitally from the current records, which are shown in Fig. 1*A*. Both a transient and a sustained outward current are evoked on depolarizing from a holding potential of  $-100$  mV (lower current records, Fig. 1*A*), but the transient component is absent on stepping to the same potentials from  $-40$  mV (upper current traces, Fig. 1*A*). The transient current activates at more negative voltages than the sustained current and can be recorded by itself at such voltages. Some cells lacked much sustained current so that an A-current could be activated apparently by itself, as in Fig. 1*B*.

The two outward currents could also be separated on a pharmacological basis, since the transient component was selectively blocked by 4-AP. Figure 1*B* shows currents evoked in a neurone held at  $-100$  mV. The transient current was reduced by puffer application of 2.5 mM-4-AP over the cell soma. In five cells the A-current was reduced by  $19.3 \pm 4.5\%$ , while the sustained current was unaffected.

*Whole-cell activation and inactivation curves*

The voltage dependence of activation and inactivation of A-current was examined and the results from three cells are shown in Fig. 2. The relation for inactivation was determined by setting the holding potential at various levels and stepping to  $+10$  mV. The relation for activation was plotted by holding at  $-120$  mV, in order to remove inactivation fully, and then stepping to progressively more positive potentials. The conductance was computed assuming a reversal potential of  $-80$  mV (see below) and a linear instantaneous current-voltage relation. The results are plotted normalized to the conductance at  $+20$  mV. The inactivation curve was well fitted by a Boltzmann distribution of the form:

$$G_o = \frac{G_{\max}}{1 + \exp [(V - V')/k]}, \quad (1)$$

with  $k = 10.5$  mV and  $V' = -92.5$  mV. In contrast, the activation curve was not well fitted by a Boltzmann, but this finding may be explained by the rectification shown by unitary current-voltage relations (see below and inset to Fig. 2).

*Properties of unitary currents**Unitary A-currents*

Unitary A-currents were observed in approximately half the membrane patches from which on-cell recordings were made (110 out of 216 patches). Channels activated rapidly on depolarization from holding potentials negative to  $-60$  mV and

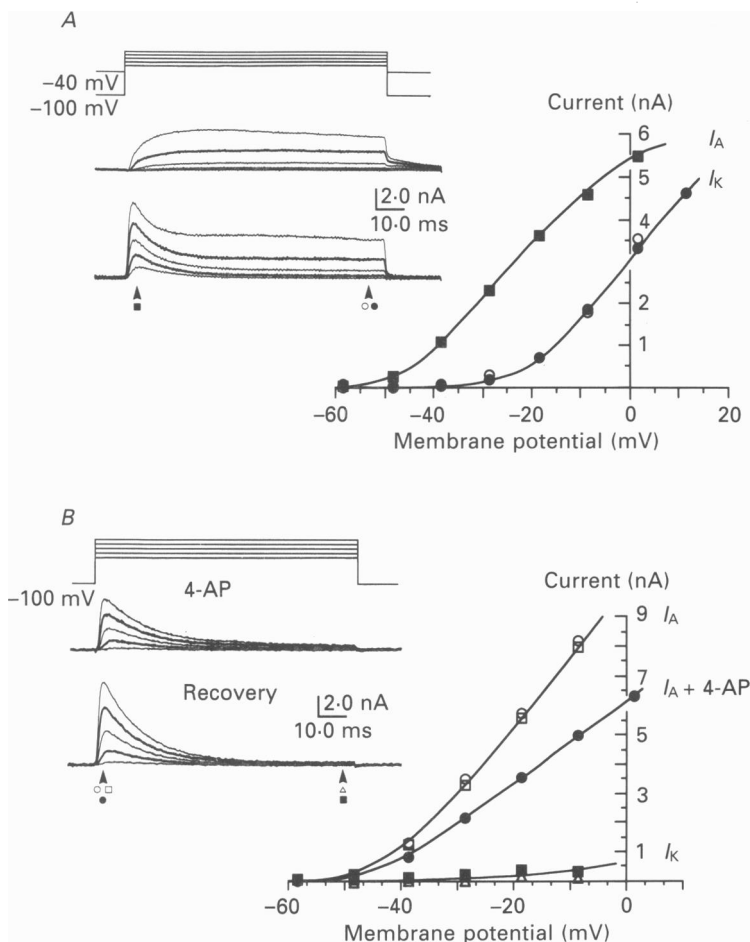


Fig. 1. Transient and sustained outward potassium currents in locus coeruleus neurones. Voltage clamp recordings were made using the whole-cell recording mode of the patch clamp. Outward currents were evoked by step depolarizations from a holding potential of either -40 or -100 mV. Voltage steps increased progressively in increments of 10 mV. The current records are single traces filtered at 1 kHz, and have leakage currents and capacity transients subtracted digitally. Temperature, 30 °C. A correction for a junction potential of -8.5 mV has been made on the current-voltage relations. *A*, the inset shows the outward current evoked from a holding potential of -40 mV (above) and -100 mV (below). The current evoked from -40 mV activates slowly and is sustained during the depolarizing pulse. The current evoked from -100 mV activates rapidly and inactivates within approximately 30 ms to a sustained level. The vertical arrow-heads and symbols show the times at which currents were measured for the current-voltage relations. The current-voltage relations show sustained currents activated from -40 (●) and from -100 mV (○). The transient current ( $I_A$ , ■) is plotted as the difference between currents measured from holding potentials of -40 and -100 mV. *B*, the transient current is reduced by 4-aminopyridine (4-AP); 2.5 mM-4-AP was applied by pressure ejection onto the cell soma. Open symbols show control (○) and recovery (□) current-voltage relations, and the filled symbols (●, ■) show currents measured during 4-AP application. 4-AP reduced transient outward current by 36%. The experimental records show the effect of stepping from -100 to between -40 and 0 mV, during (middle) and after (bottom) application of 4-AP.

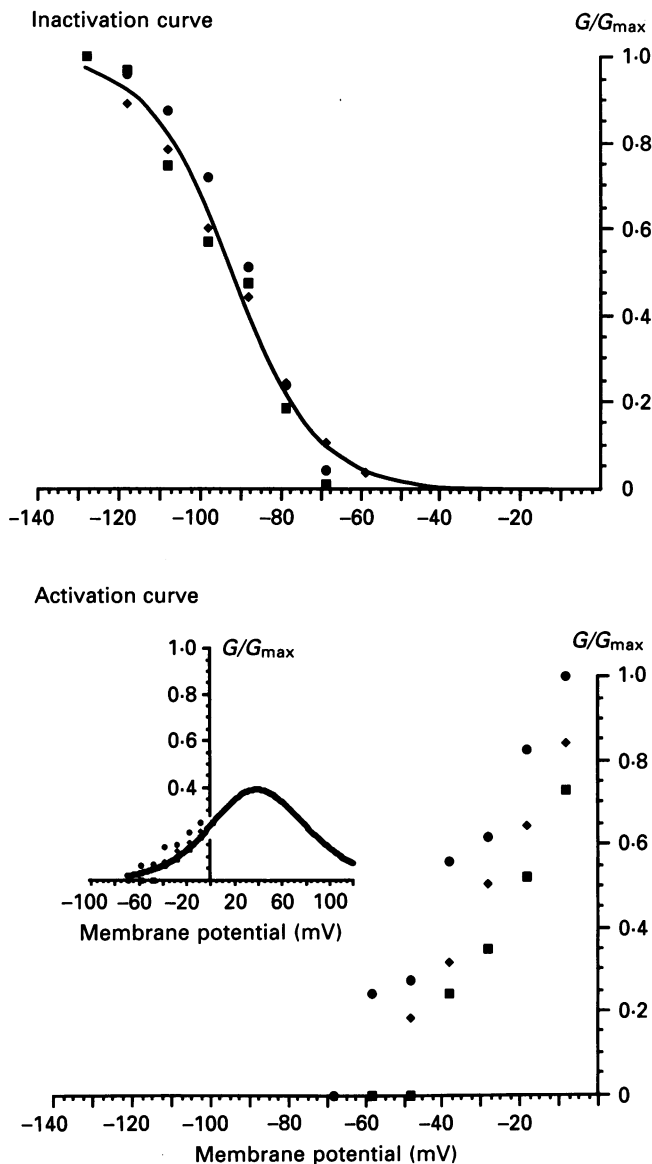


Fig. 2. Activation and inactivation of whole-cell A-current. The filled symbols give results from three cells. Inactivation (above): the membrane potential was clamped at holding potentials from  $-130$  to  $-40$  mV and stepped to  $0$  mV, and the transient current is plotted as the fraction of that evoked from a holding potential of  $-130$  mV. The results plotted have been corrected for a junction potential of  $-8.5$  mV. They are fitted by eqn (1) of the text with  $k = 10.5$  mV and  $V' = -92.5$  mV.

Activation (below): the membrane potential was stepped from a holding potential of  $-120$  mV to progressively more positive levels. The currents evoked were converted to conductances assuming a linear instantaneous current-voltage relation and a reversal potential of  $-80$  mV and are plotted as the fraction of that measured at  $+20$  mV. The inset shows the experimental points fitted by a modified Boltzmann relation using identical parameters to those for the single channel data (see Fig. 4) and assuming voltage-dependent ionic blockage by intracellular  $Mg^{2+}$  and  $Na^+$  as described in the text (see Discussion).

then rapidly inactivated during the voltage step. Recordings were made with either 140 mM or 3 mM-K<sup>+</sup> in the pipette. The resting potential of neurones was  $-61.4 \pm 6.3$  mV ( $n = 16$ ), measured by breaking into the cell at the end of recording.

An example of such unitary currents, recorded with a pipette [K<sup>+</sup>] of 140 mM, is shown in Fig. 3*A*, the patch containing two active channels. The patch was held 40 mV negative to the resting potential, and depolarizing steps were applied at 0.5 Hz. The upper part of Fig. 3*A* shows the channel openings that occur on stepping by 180 mV (to a membrane potential of approximately +80 mV). The unitary current, measured from the amplitude histogram shown in Fig. 3*A*, is  $1.33 \pm 0.18$  pA. With smaller depolarizations (lower part of Fig. 3*A*), the open state probability of the channels decreased and the latency to the first opening increased. At the voltage shown in the lower part of Fig. 3*A*, stepping by 60 mV (i.e. to a membrane potential of approximately -40 mV, which is negative to the reversal potential for potassium), the current is inward with an amplitude of  $-1.03 \pm 0.14$  pA. Although the great majority of openings were to this level, a subconductance state was also observed. This and other substates are discussed below.

The ensemble averages of 100 records are plotted for the same patch in Fig. 3*B* for voltage steps 180, 140, 80, and 60 mV positive to the holding potential. The time course of these ensemble averages is similar to that of macroscopic currents under whole-cell recording (Fig. 1). The unitary current-voltage relation is not linear (Fig. 3*C*), and outward currents are smaller than expected. The unitary slope conductance at negative voltages is 44.5 pS in this case.

#### *Voltage dependence of activation and inactivation of unitary currents*

The steady-state dependence on voltage of activation and inactivation was measured in four on-cell patches. The results from one such patch, containing a single active channel, are shown in Fig. 4. Here the open state probability,  $P_o$ , is plotted against the change in membrane potential from the resting level. The relations for activation and inactivation were well fitted by Boltzmann expressions of the form:

$$P_o = \frac{P_{\max}}{1 + \exp[(V - V')/k]}, \quad (2)$$

where  $V$  is the voltage relative to the resting potential,  $V'$  is the voltage at which  $P_o$  is 0.5 of  $P_{\max}$ , and  $k$  gives the steepness of the voltage dependence of  $P_o$ . For the patch of Fig. 4,  $V'$  and  $k$  were found to be 86.6 and -22.4 mV, respectively, for activation. For inactivation, values of -33.2 and 10.2 mV, respectively, were found.

Mean values for  $V$  and  $k$  were found to be  $71.9 \pm 11.8$  mV and  $-17.1 \pm 3.6$  mV respectively for activation. For inactivation, the mean values of  $V$  and  $k$  were  $-29.4 \pm 3.8$  mV and  $8.6 \pm 1.9$  mV. The maximum value for  $P_o$ , measured in seven patches, was  $0.78 \pm 0.17$ . We made similar measurements on only one excised inside-out patch, measuring the relation between steady-state inactivation and membrane potential, with  $V' = -90.0$  mV and  $k = 10.0$  mV. These values are in agreement with those obtained in on-cell recording, given that cellular resting potentials were approximately -60 mV.

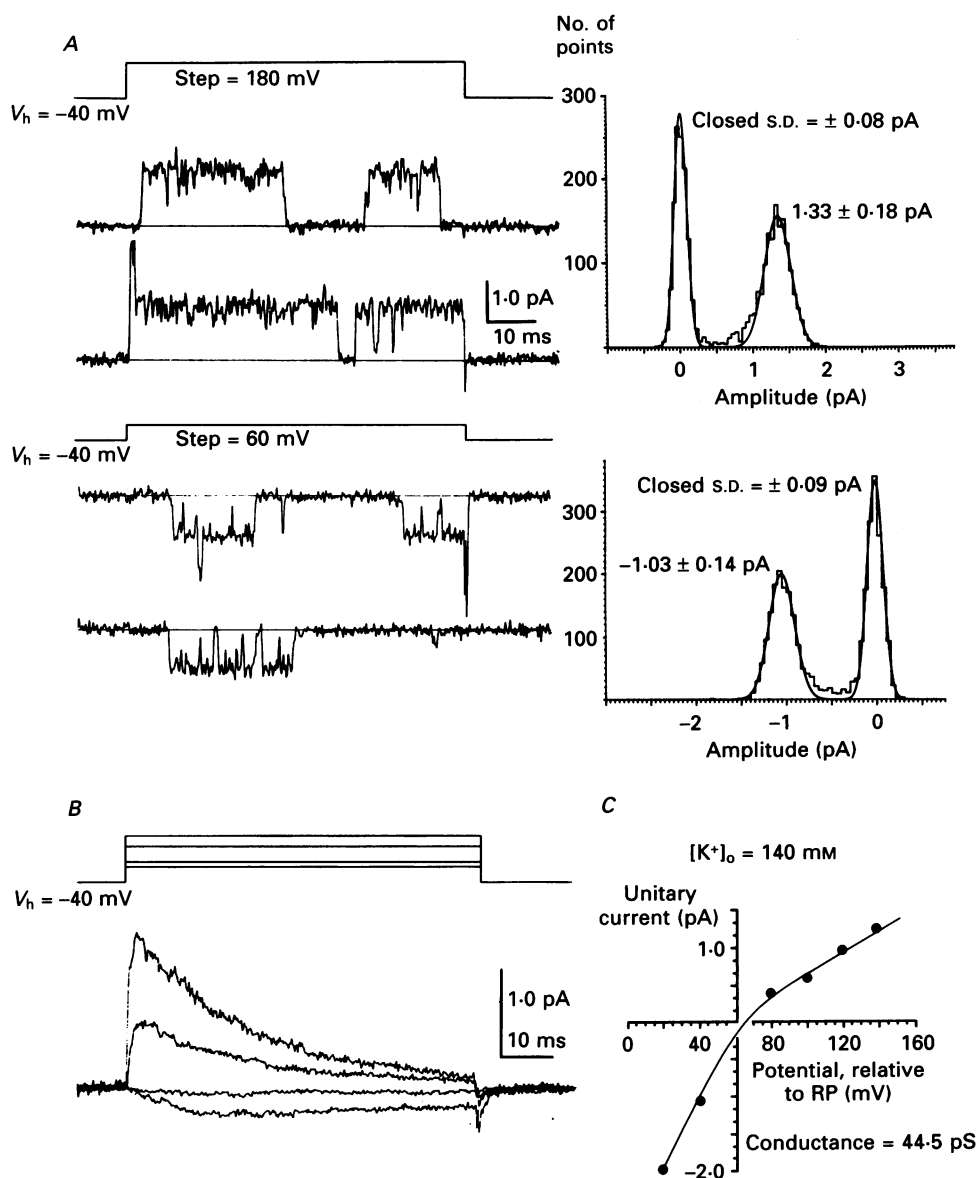


Fig. 3. Unitary A-currents observed in cell-attached membrane patches. The patch electrode contained 140 mM-K<sup>+</sup>, and the patch was held 40 mV negative to the resting membrane potential. *A*, unitary A-currents recorded (above) under a 180 mV depolarization (i.e. to a membrane potential of approximately +60 mV) and (below) under a 60 mV depolarization. Two channels are present in the patch. The amplitude histograms, chosen from records where only one channel was open, indicate that unitary current was 1.33 pA under the 180 mV depolarization and -1.03 pA under the 60 mV depolarization. *B*, ensemble averages of currents recorded under depolarizations of (from top to bottom) 180, 140, 60 and 80 mV. 100 sweeps were averaged in each case. *C*, unitary current-voltage relation, plotting single channel current (pA; ordinate) against membrane potential, relative to the resting potential (RP; in mV; abscissa). The unitary current was measured from amplitude histograms such as those shown in *A*.

*Runs analysis of channel openings*

A number of authors (eg. Horn, Vandenburg & Lange, 1984; Standen, Stanfield & Ward, 1985) have shown that the openings of voltage-activated ion channels under repeated depolarizing pulses occur in a non-random manner, such that failures to

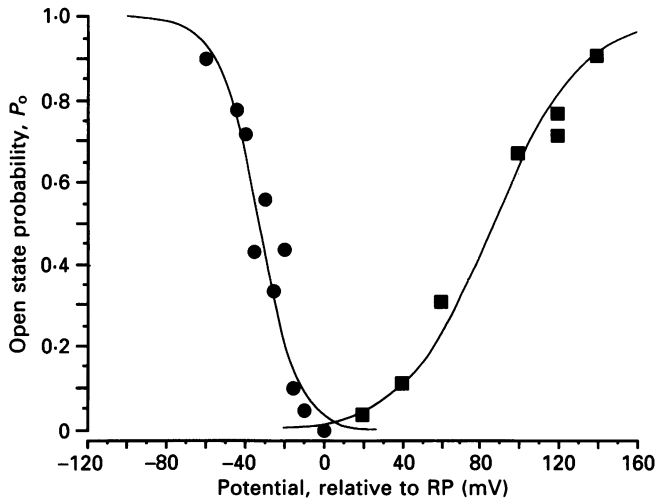


Fig. 4. Activation and inactivation of unitary A-currents, cell-attached patch recording. The open state probability,  $P_o$ , is plotted against patch potential, as measured relative to the cell resting potential (RP). The relation between steady-state inactivation and membrane potential (●) is fitted with a Boltzmann relation (eqn (2) of text) with  $P_{\max} = 1$  in this instance,  $k = 10.2$  mV and  $V' = -33.2$  mV. Activation (■) is fitted with a similar Boltzmann relation with  $P_{\max} = 1$ ,  $k = -22.4$  mV and  $V' = 86.6$  mV.

respond to the depolarizing pulse tend to occur in groups. This grouping has been associated with slow steps in the inactivation of the ion channel (Horn *et al.* 1984; Standen *et al.* 1985).

We have counted runs of channel openings, where, in a series of  $n$  sweeps, a run is formed from consecutive sweeps in which channel openings occur each sweep *or* in which they fail to occur. The expected number of runs is  $2np(1-p)$  if the response to successive voltage pulses is random, where  $p$  is the probability of the channel opening at least once in response to the depolarizing pulse, and where  $(1-p)$  is the probability that the channel fails to respond. If the observed number of runs is  $R$ , one may evaluate,

$$Z = \frac{R - 2np(1-p)}{2\sqrt{np(1-p)}}$$

(eqn 2.9 of Gibbons, 1971) where  $Z$  is a standardized random variable with mean 0 and standard deviation 1. When  $Z$  is large and negative, channel openings and failures to open in response to successive sweeps are significantly grouped.

Some evidence of grouping occurs in many measurements, but grouping becomes more marked when  $p$  is reduced by increasing steady-state inactivation. There may

be little sign of grouping when  $p$  is reduced by reducing activation under circumstances where there is little steady-state inactivation.

In the experiment of Fig. 4, on stepping from a holding potential 60 mV negative to the resting potential to 120 mV positive to resting, ninety-four out of ninety-nine sweeps elicited channel openings. Ten runs were observed and the expected number was 9.6.  $Z$  evaluates to 0.42, consistent with openings occurring randomly. When the holding potential was reduced to only 25 mV negative to the resting potential, depolarization to the same potential produced openings on only 73 sweeps out of 200. Now the number of runs observed was only 49, against an expected number of 97.1.  $Z$  has a value  $-7.34$ , and since the probability of the number of runs observed in this instance occurring by chance may also be shown to be  $3.9 \times 10^{-12}$  (Gibbons, 1971), the events were distributed in a non-random fashion.

However, when the holding potential was returned to 60 mV negative to the resting level, largely removing inactivation, stepping to 20 mV positive to the resting potential now produced openings during 35 sweeps out of 100. The observed number of runs was 47, compared with an expected number of 45.5;  $Z$  was 0.33, consistent with openings occurring randomly, the probability of observing the number of runs by chance being 0.15.

Thus when  $p$  is reduced to 0.37 by increasing steady-state inactivation, openings and failures to open are grouped, but when  $p$  is reduced to 0.35 by reducing activation while keeping inactivation at a minimum, openings and failures to open occur randomly. We conclude that the non-random behaviour is indeed associated with slow steps in the inactivation process.

#### *Dependence on $[K^+]_o$*

The reversal potential and unitary conductance of channels depended on the concentration of  $K^+$  used in the pipette. In Fig. 5, records, ensemble averages and unitary current-voltage relations are plotted for recordings with a pipette  $[K^+]$  of 3 mM. Figure 5A shows unitary currents obtained on stepping by 140 and 60 mV from a holding potential 40 mV negative to the resting potential, together with their amplitude histograms. The unitary current-voltage relation shows marked rectification, with a negative slope conductance at positive voltages.

With a pipette  $[K^+]$  of 140 mM, currents reversed at a membrane potential  $65.7 \pm 4.1$  mV ( $n = 6$ ) positive to the resting potential (i.e. close to zero in terms of absolute voltage). With a pipette  $[K^+]$  of 3 mM, currents reversed at a potential negative to the range of voltages where  $P_o > 0$ . By extrapolation, the reversal potential was 15.3 mV negative to the resting potential in the patch of Fig. 5. Unitary conductances, measured between 20 and 40 mV positive to the resting potential, were  $40.9 \pm 2.2$  pS ( $n = 6$ ) and  $14.8 \pm 1.4$  pS ( $n = 11$ ) with the pipette  $[K^+]$  at 140 and 3 mM respectively.

#### *Substates of the channel*

Although the great majority of channel openings were to the levels described above, subconductance states were also observed. The most easily identified substate, measured in five patches, was to  $0.55 \pm 0.04$  ( $n = 5$ ) of the amplitude of the

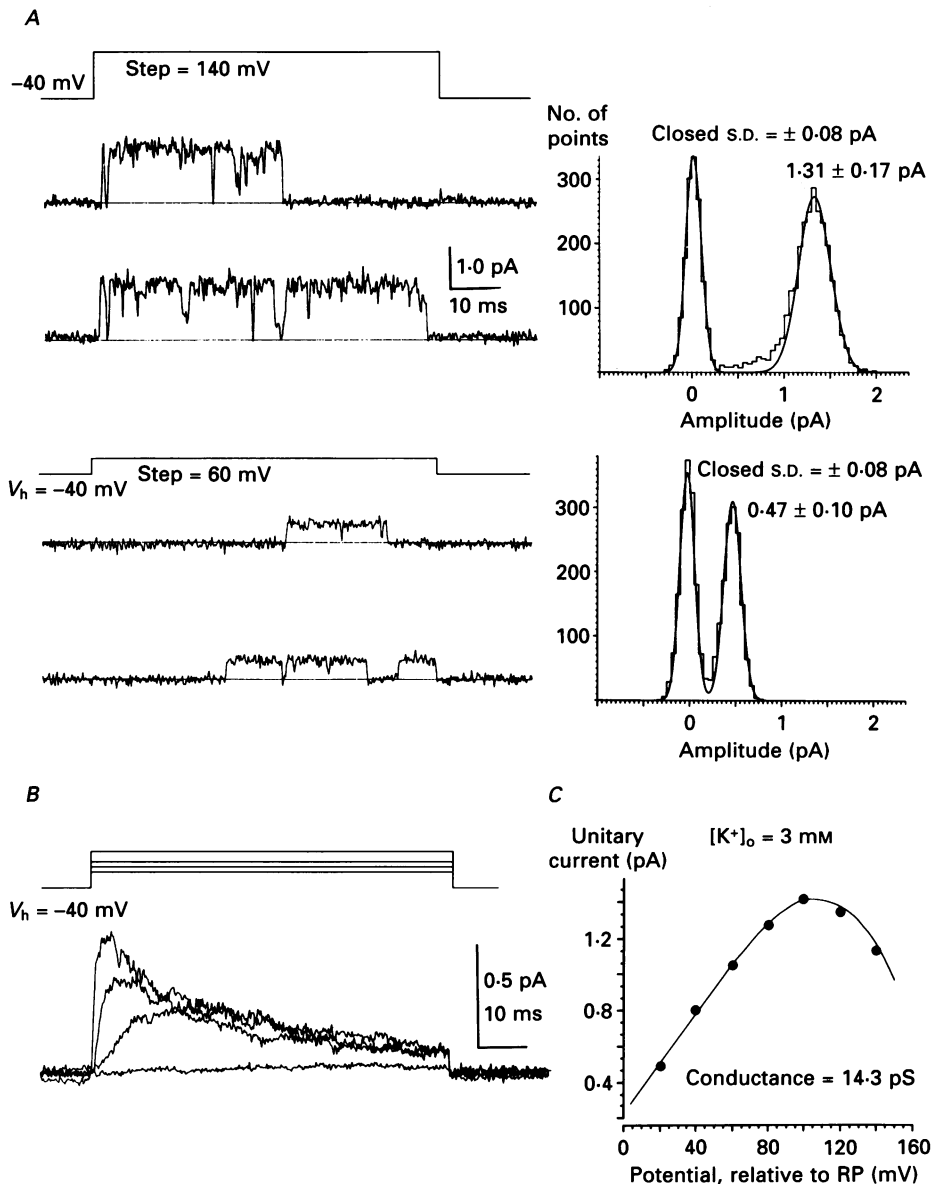


Fig. 5. Unitary A-currents recorded in the on-cell configuration, using physiological (3 mM)  $[K^+]_o$ . The membrane potential was held 40 mV negative to the resting potential. *A*, unitary currents recorded under a 140 mV depolarization (i.e. to a membrane potential of approximately +40 mV; above) and under a 60 mV depolarization (i.e. to a membrane potential of approximately -40 mV; below). The amplitude histograms, chosen from records where only one channel is open, show the unitary current amplitude was 1.31 pA under the 140 mV depolarization and 0.47 pA under the 60 mV depolarization. *B*, ensemble averages for unitary currents. The current traces show ensemble averages of 90–100 responses to step depolarizations of (from top to bottom) 140, 100, 80 and 60 mV. *C*, the current–voltage relation plots unitary current amplitude (ordinate) against membrane potential (abscissa), relative to the resting potential. The current–voltage relation shows rectification, of greater magnitude at physiological than at high  $[K^+]_o$  (see also Fig. 3).

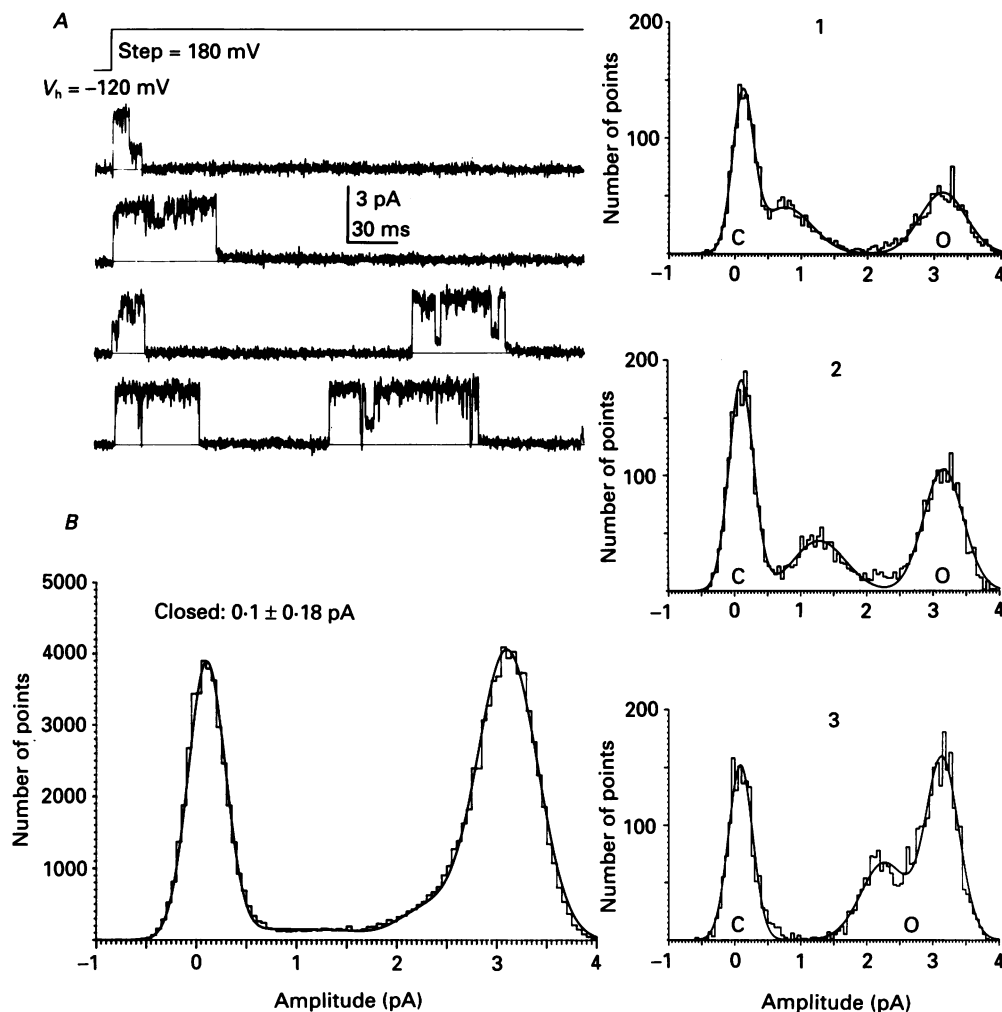


Fig. 6. Substates measured in an excised, inside-out membrane patch, with physiological ( $3$  mM)  $[K^+]_o$ , containing a single channel. *A*, unitary current records obtained by depolarizing from a membrane potential of  $-120$  to  $+60$  mV. The records are selected to show substates of different amplitudes. Amplitude histograms of such sections of records (right of figure) show the presence of substates whose amplitude is  $0.7 \pm 0.3$  pA (histogram 1),  $1.3 \pm 0.3$  pA (histogram 2), and  $2.2 \pm 0.3$  pA (histogram 3), while the current amplitude for the fully open channel is  $3.0 \pm 0.3$  pA. In each histogram, the closed level is indicated at C, while the fully open level is indicated at O. *B*, amplitude histogram of all current records, illustrating the probability of occupying the various substates, using amplitude and variance of the Gaussians used to fit the histograms at the right of the figure. The best fit was obtained assuming that the respective substates are occupied  $0.03$ ,  $0.03$ , and  $0.09$  of the time spent open.

fully open state. However, careful measurement permits identification of three substates (Fig. 6), and occupancy of each of them depends on voltage (Fig. 7). The experiment of Fig. 6 was carried out with an excised, inside-out patch, where channel currents are larger (see below) owing to removal of blockage by intracellular  $Mg^{2+}$

and  $\text{Na}^+$ , using physiological  $[\text{K}^+]_o$ . The experiment of Fig. 7 used cell-attached recording, with high  $[\text{K}^+]_o$ .

Figure 6*A* shows recordings where substates are reasonably prominent during a depolarization from a holding potential of  $-120$  mV (membrane potential; excised

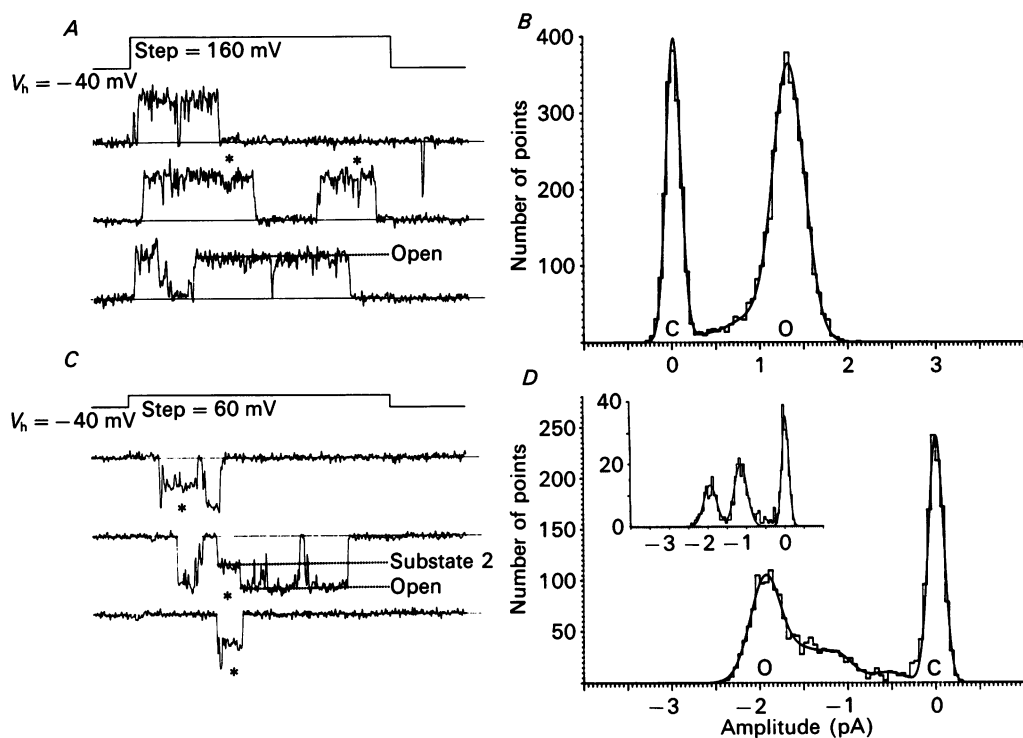


Fig. 7. Substates measured in a cell-attached patch with high (140 mM)  $[\text{K}^+]_o$ . Occupancy of substates is voltage dependent. *A*, records of unitary currents under a 160 mV depolarization from a holding potential 40 mV negative to the resting potential. \* shows a substate whose amplitude is approximately 0.7 of the fully open level. *B*, amplitude histogram formed as in Fig. 6, by constructing histograms from sections of record where occupancy of one substate is frequent, and using the amplitude and variance found to find the best fit to all current records. Substates had amplitudes of  $0.35 \pm 0.18$  pA,  $0.70 \pm 0.18$  pA, and  $0.95 \pm 0.18$  pA, compared with the fully open level of  $1.35 \pm 0.18$  pA. The substates were found to be occupied 0.02, 0.04 and 0.06 of the time spent open. *C*, records of unitary currents under a 60 mV depolarization from a holding potential 40 mV negative to the resting potential. \* shows a substate whose amplitude (approximately 0.6 of the fully open level) is shown by the horizontal dashed line. *D*, amplitude histogram formed as in Fig. 6 and in part *B* of this figure. The inset shows the fit to selected records containing a substate whose amplitude is approximately 0.6 of the fully open level. The histogram of all current records at this potential show substates whose amplitude are 0.28, 0.58 and 0.78 of the fully open level occupied 0.06, 0.18 and 0.14 of the time spent open.

patch) to  $+60$  mV. Below are shown amplitude histograms for pieces of record that contain currents when the channel is fully closed or open either fully or to one only of the three substates identified. These substates have amplitudes that are 0.23

(histogram 1), 0.43 (histogram 2), and 0.73 (histogram 3) of the fully open level. Figure 6*B* shows the amplitude histogram for all records, fitted with the Gaussians needed to fit individual substates. When the channel is not closed it spends 0.85 of its time fully open and 0.03, 0.03, and 0.09 of the time open to each of the three substates in their ascending order of size.

The increase in unitary amplitude in excised patches makes identification of substate behaviour easier. But the presence of substates is not a result of patch excision and essentially the same result is seen in cell-attached recording (Fig. 7). Figure 7*A* and *B* shows that substates may be identified under a 160 mV depolarization from a holding potential 40-mV negative to the resting potential (i.e. to a membrane potential of approximately +100 mV). These had amplitudes 0.26, 0.52, and 0.70 of the fully open level, and when open the channel spent 0.02, 0.04, and 0.06 of its time at each level.

Occupancy is, however, strongly dependent on voltage and substates were occupied more at negative membrane potentials (Fig. 7*C* and *D*). Substates whose amplitudes were 0.28, 0.58, and 0.78 of the fully open were identified under a step of 60 mV from the holding potential. These substates were occupied 0.06, 0.18, and 0.14, respectively, of the time the channel was open. The increase in relative occupancy of substates at negative voltages is evident from inspection of the amplitude histograms of Fig. 7*B* and *D*.

### *Kinetic properties of A-current channels*

#### *Channel kinetic behaviour*

We have attempted a preliminary analysis of channel kinetic behaviour. Given the presence of substates, it was found easiest to measure openings and closures as current crossed a cursor set at 30%, rather than 50%, of the fully open level. The channel was considered open when it was in a substate.

Figure 8*A* shows records from a patch containing a single active channel, in an excised, inside-out membrane patch, held at -120 mV and stepped by 180 mV to +60 mV, together with the ensemble average of the unitary currents. The distribution of open times (Fig. 8*B*) is best fitted with a single exponential whose mean, uncorrected for missed closures, was 15.3 ms. Correction for missed closures (Colquhoun, 1987) gave a mean time of 12.0 ms.

The distribution of first latencies (Fig. 8*C*) increases with an initial delay and appears to be composed of the sum of at least three exponential elements. Closed time distributions (Fig. 8*D* and *E*) also contained at least three exponentials and the distribution of Fig. 8 was best fitted with four, with time constants of 0.25, 1.52, 32.4, and 123.3 ms. The time constants and relative areas for four on-cell and two excised channels are shown in Table 2 for steps to approximately +40 mV.

#### *Voltage dependence of the open and closed states*

Recordings of sufficient duration to allow the collection of records over a range of voltages were achieved in only two patches containing single channels, one on-cell and one-inside out. The results are essentially similar in each case. Open and closed time distributions for the excised patch are shown in Fig. 9. The open time

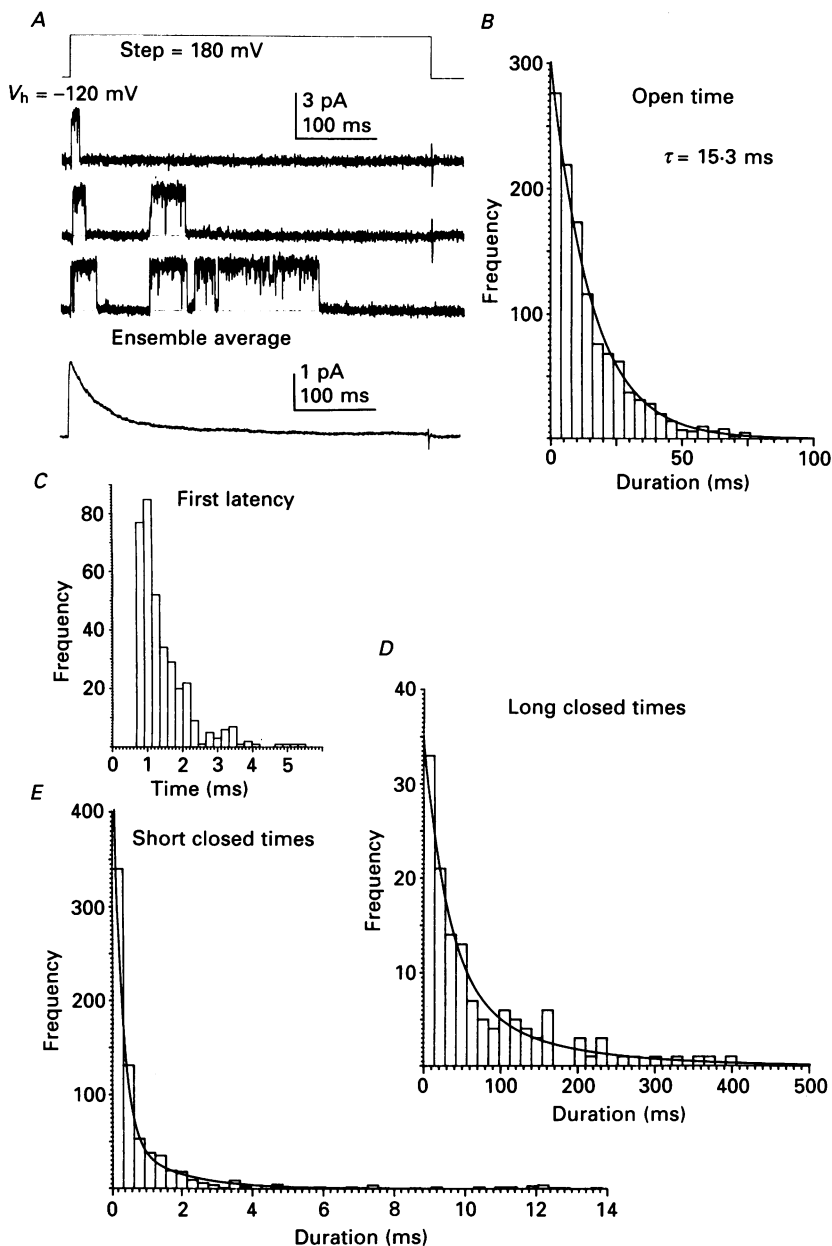


Fig. 8. Kinetic behaviour of channels carrying A-current. *A*, unitary currents, recorded from a single channel patch, which was excised in the inside-out configuration. The holding potential was  $-120$  mV and the voltage step is to  $+60$  mV. The ensemble average was formed from 430 sweeps such as those shown. *B*, open time histogram formed as described in the text, treating substates as open. Given that proviso, the open times are distributed according to a single exponential, with  $\tau_{\text{open}} = 15.3$  ms at this potential. *C*, latency to first opening, measured from the start of the depolarizing pulse to the start of the first channel opening. The first latency distribution rises with a delay as expected if the channel runs through a series of closed states before opening. *D* and *E*, closed times are distributed according to multiple exponentials. Fitting the longest exponentials gave

distributions are plotted on the left on stepping from the holding potential of  $-100$  mV to 0,  $+20$  and  $+60$  mV. In each case, the distribution is fitted with a single exponential. The mean open time increases with depolarization, a finding confirmed with the on-cell patch, where the voltage was stepped by 40, 80 and 100 mV positive to the resting potential. The respective mean open times were 6.6, 11.2 and 14.0 ms.

TABLE 2. Open and closed times for channels carrying A-current single channel patches

Open times			Closed times		
Step* (mV)	$\tau_{\text{open}}$ (ms)	$\tau_{\text{closed}(1)}$ (ms)	$\tau_{\text{closed}(2)}$ (ms)	$\tau_{\text{closed}(3)}$ (ms)	$\tau_{\text{closed}(4)}$ (ms)
Cell-attached patches					
100	14.6	0.25 (0.71)	1.82 (0.25)	25.0 (0.04)	
100	18.1	0.22 (0.59)	1.37 (0.33)	32.0 (0.08)	
100	14.0	0.20 (0.90)	2.47 (0.08)	20.6 (0.03)	
100	18.2	0.13 (0.80)	1.24 (0.13)	25.9 (0.07)	
Mean	16.2 ± 2.2	0.20 ± 0.05 (0.75 ± 0.13)	1.72 ± 0.55 (0.20 ± 0.11)	25.9 ± 4.70 (0.05 ± 0.02)	
Excised, inside-out patches					
40	12.9	0.33 (0.65)	1.42 (0.20)	19.0 (0.02)	142 (0.13)
40	15.3	0.25 (0.50)	1.52 (0.34)	32.4 (0.07)	123 (0.09)

\* The voltage step is expressed relative to the resting potential for cell-attached patches and in absolute terms for the excised patches. The values in parentheses for closed times are the relative areas of each component.

The latency to first opening is plotted for each voltage on the right of Fig. 9, the insets showing the shorter (open bars) and the longer (filled bars) closed times. As expected from a channel gated by voltage, the first latency distribution shows a strong dependence on membrane potential. In Fig. 9, the median value for the first latency decreases from 4.9 ms at 0 mV to 1.5 ms at  $+20$  mV and 1.0 ms at  $+60$  mV.

Three elements to the closed time distribution were fitted with values of 0.20, 2.5 and 24.6 ms at  $+100$  mV; 0.23, 3.5 and 15.9 ms at  $+80$  mV; and 0.26, 2.9 and 12.4 ms at 40 mV. Little voltage dependence is seen for either of the two fastest closed durations (right, middle plot), though the time constant of the third closed duration does show some voltage dependence.

Insufficient records were made to allow fitting of the longest element of the closed time distribution, but the data presented in the upper inset (filled bars) indicates the presence of some very long closures. The slowest component of the closed time histogram may represent visits to inactivated states, rather than returns to other shut states occupied on the way to opening. It is likely that the closed time distribution contains other brief elements than those we have been able to identify.

Preliminary analysis of bursts of channel openings at two voltages in the excised patch indicate little voltage dependence in the mean number of bursts per trace ( $1.54 \pm 0.89$  at  $+60$  mV;  $1.36 \pm 0.70$  at 0 mV; the critical closed duration used to

---

values for time constants ( $\tau_3$  and  $\tau_4$ ) of 32.4 and 123.3 ms. The excess of short closures that results was fitted ( $E$ ) with exponential functions with time constants ( $\tau_1$  and  $\tau_2$ ) of 0.25 and 1.52 ms.

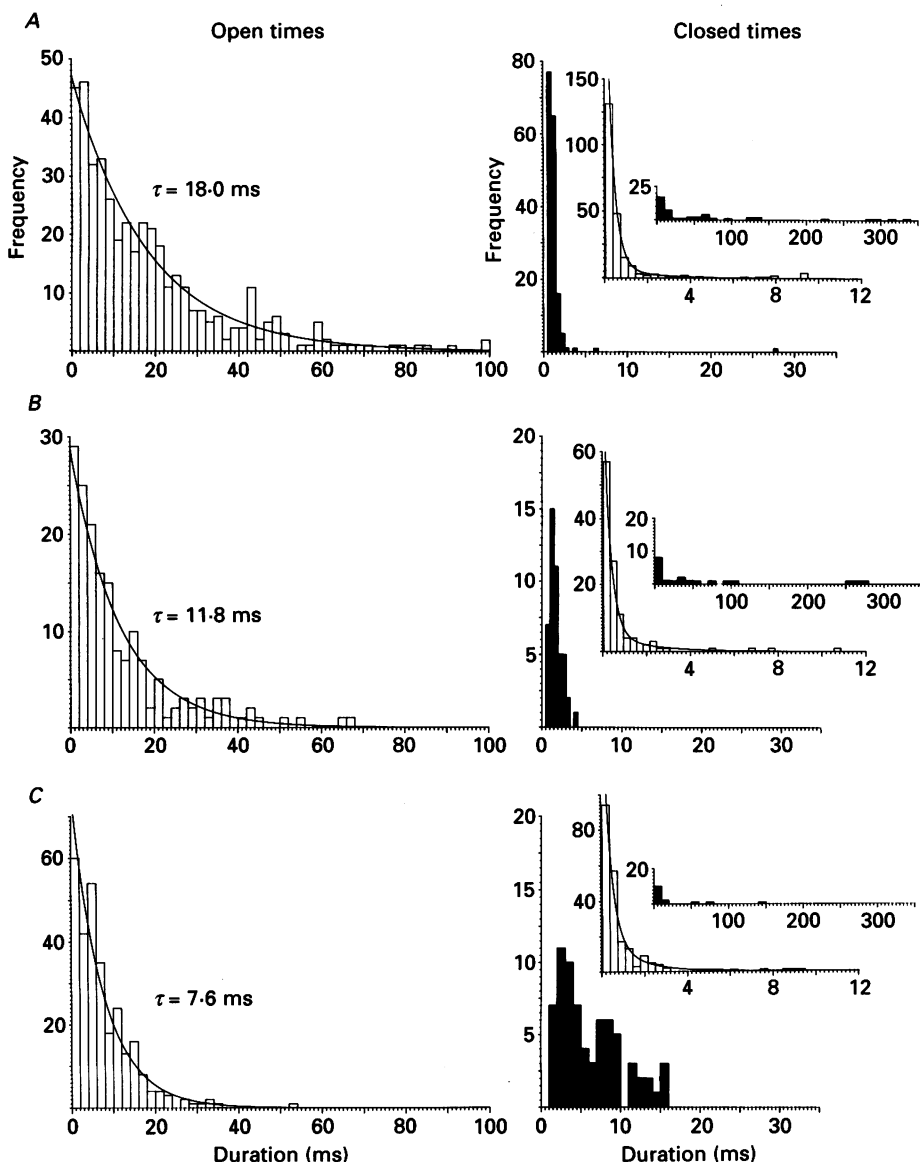


Fig. 9. Voltage dependence of open and closed durations in an excised inside-out patch. The patch was held at  $-100$  mV and stepped positive for 450 ms at 0.5 Hz. Frequency distributions for open times are plotted on the left and for closed times on the right. The closed times are plotted on three axes; top, long closed times (filled bars to histogram); middle, short closed times (open bars); bottom, first latency (filled bars). The short closed times were fitted with two exponentials (see Table 2), no attempt was made to fit the longest closed times because of their small number. The open times were fitted with a single exponential. *A*, step to  $+60$  mV,  $\tau_{\text{open}}$  is 18.0 ms and the median time to first opening is 1.0 ms. *B*, step to  $+20$  mV,  $\tau_{\text{open}}$  is 11.8 ms, with the median time to first opening of 1.5 ms. *C*, step to 0 mV,  $\tau_{\text{open}}$  is 7.6 ms, and the median time to first opening is 4.9 ms.

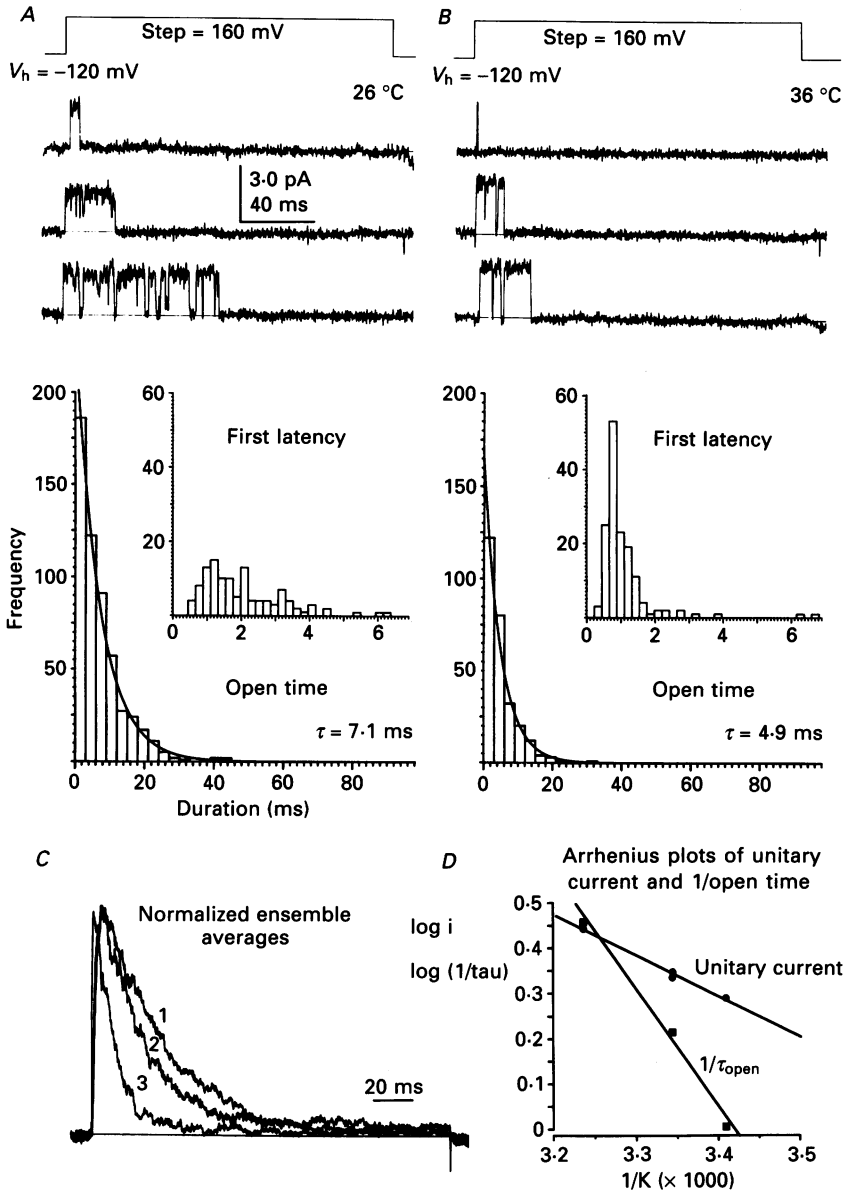


Fig. 10. Effects of temperature on kinetic behaviour; excised, inside-out membrane patch. *A* and *B*, unitary currents obtained on depolarizing from a holding potential of -120 to +40 mV at 26 (*A*) and 36 °C (*B*). Below in each case are shown the distribution of channel open times and of first latencies. *C*, normalized ensemble averages of currents obtained in response to the depolarizations shown in *A* and *B* at 20 (1), 26 (2) and 36 °C (3). The ensemble averages are of 100 sweeps in each case, and are normalized to the same amplitude. The decays were fitted with time constants of 31.8, 23.5, and 10.0 ms respectively. *D*, an Arrhenius plot giving unitary current amplitude and the reciprocal of the mean open time ( $1/\tau_{open}$ ), after correction for missed closings (log scale, ordinate), are plotted against temperature<sup>-1</sup> ( $1/K$ , abscissa). For unitary current (●): slope = -896.9, activation energy ( $E$ ) = 17.17 kJ mol<sup>-1</sup>. For  $1/\tau_{open}$  (■): slope = -2559.5,  $E$  = 48.99 kJ mol<sup>-1</sup>.

delineate bursts was chosen to be 0.9 ms in each case). However, the mean number of openings per burst was voltage dependent, changing from 1.82 at +60 mV to 2.95 at 0 mV.

#### *Temperature dependence of channel kinetics*

Figure 10 shows an experiment investigating temperature dependence, using an excised, inside-out membrane patch, containing a single active channel studied at 20, 26, and 36 °C. Figure 10*A* and *B* shows records under a depolarization to +40 mV, measured at 26 °C (*A*) and 36 °C (*B*), together with the distributions of open times and first latencies, and the ensemble averages of currents (Fig. 10*C*) normalized to have the same peak amplitude. Temperature has a marked effect on channel behaviour, altering unitary current amplitude, open time, the time-to-peak of the ensemble average and the first latency, and the time course of inactivation of currents.

We have made Arrhenius plots of unitary current and the reciprocal of the mean open time (which will be dominated by the transition rate for leaving open to return to closed). In this patch the activation energy is 17.2 kJ mol<sup>-1</sup> for unitary current and 49.0 kJ mol<sup>-1</sup> for the reciprocal of mean open time.

#### *Rectification depends on ionic blockage: effects of Mg<sup>2+</sup> and Na<sup>+</sup>*

Unitary current-voltage relations show rectification, with the slope conductance being reduced at positive voltages (Figs 3 and 5). This rectification is more marked in 3 mM [K<sup>+</sup>]<sub>o</sub>, with a negative slope conductance at very positive voltages (Fig. 5). A similar rectification has been described by Cooper & Shrier (1985).

#### *Recordings from excised patches*

These findings are consistent with a voltage-dependent blockage of the channel by an intracellular cation. We have recorded from channels using cell-attached recording and have then excised patches in an inside-out configuration to show that the rectification can be accounted for by block by both intracellular Na<sup>+</sup> and Mg<sup>2+</sup>. After excision, the cytoplasmic surfaces of patches were exposed to a number of different solutions, and ramp changes of membrane potential were used to measure unitary current-voltage relations.

The use of a voltage ramp in recordings made on-cell and after patch excision is illustrated in Fig. 11. Here the patch pipette contained K<sup>+</sup> at 3 mM, the membrane potential was held negative to the resting potential by 40 mV, was depolarized in a step by 180 mV (that is to about +80 mV membrane potential) to activate channels, and was then returned to the holding potential at 2.25 mV ms<sup>-1</sup>. Figure 11*A* shows examples of records, as they appear after analog and digital subtraction of capacity and leakage currents, where a single channel is opening. Similar measurements made from the same patch after excision into an intracellular solution containing neither Mg<sup>2+</sup> nor Na<sup>+</sup> are shown in Fig. 11*B*. Those parts of records where a single channel is open were then ensemble averaged (and reversed in time) to give the current-voltage relation shown in Fig. 11*C*. In the on-cell recording, the current-voltage relation shows typical rectification, but in the excised patch the current-voltage relation is nearly linear, in fact with some *outward* rectification as expected when [K<sup>+</sup>]<sub>o</sub> < [K<sup>+</sup>]<sub>i</sub>.

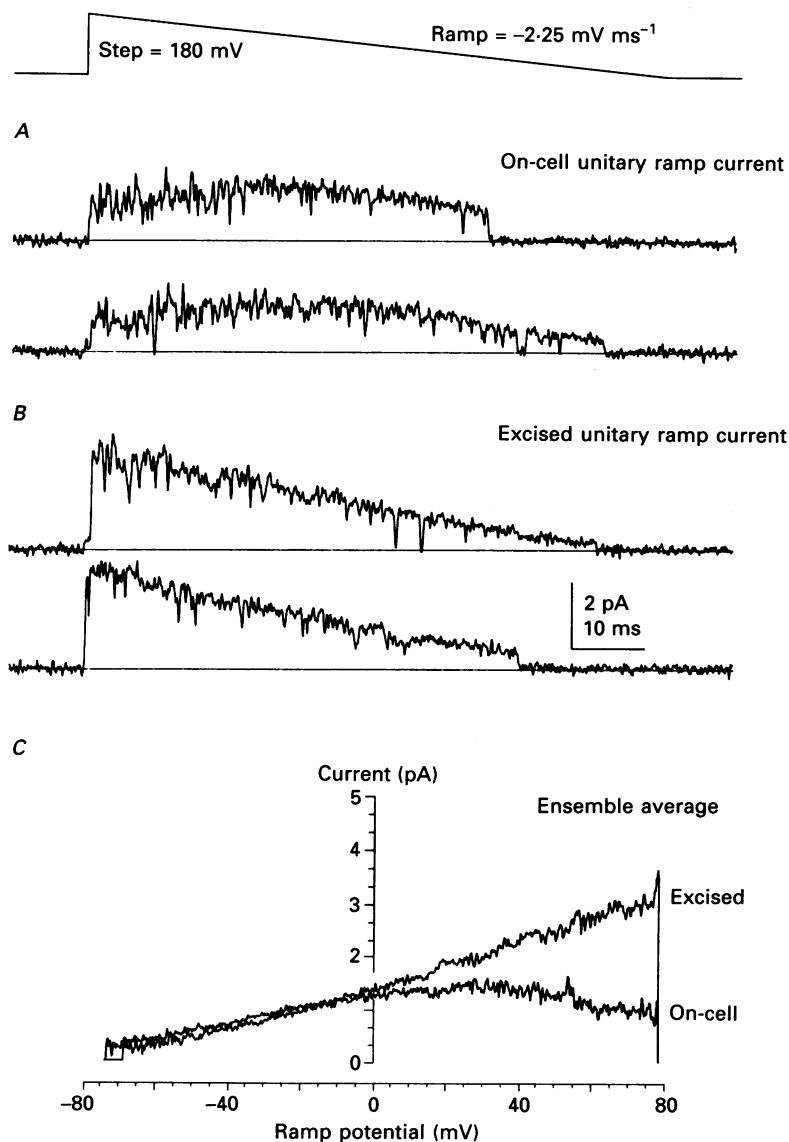


Fig. 11. Generation of unitary current-voltage relations using voltage ramps in on-cell and excised, inside-out membrane patches. A-currents are evoked by stepping to a voltage 180 mV positive to the holding potential (itself 40 mV negative to the resting potential in the case of cell-attached patches and  $-100 \text{ mV}$  in the case of excised patches), and then ramping back at  $-2.25 \text{ mV ms}^{-1}$ . *A*, unitary responses to the voltage ramp, after subtraction of leakage and capacity currents, in the on-cell patch. *B*, unitary responses to the voltage ramp after patch excision. Note the increase in current at positive voltages. Current is shown against time in *A* and *B*. *C*, the current-voltage relations constructed by ensemble averaging of parts of records where a single channel is open and plotting current against ramp membrane potential. Note that patch excision abolishes rectification of the current-voltage relation, if, as here,  $\text{Mg}^{2+}$  and  $\text{Na}^+$  are absent from the internal solution.

Figure 12*A* again shows the effect on the current–voltage relation of excising the patch into an artificial intracellular fluid containing neither  $\text{Na}^+$  nor  $\text{Mg}^{2+}$ . The mean slope conductance was  $17.8 \pm 1.8$  pS ( $n = 16$ ) and the reversal potential, measured by extrapolation, was  $-80.0 \pm 3.6$  mV with  $[\text{K}^+]_i = 140$  mM and  $[\text{K}^+]_o = 3$  mM.

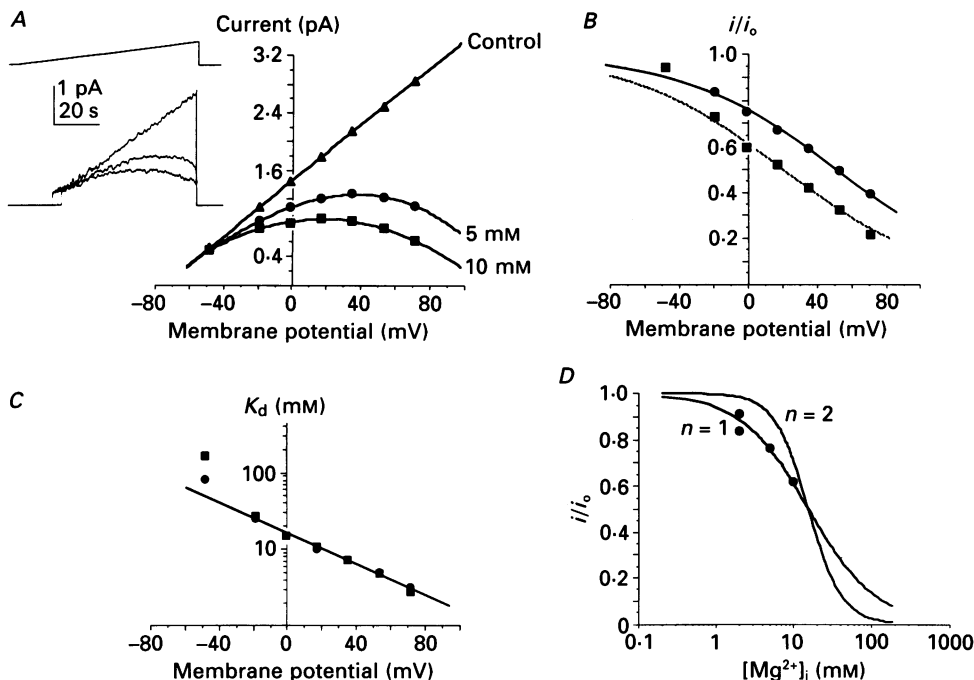


Fig. 12. Voltage-dependent block of A-current by intracellular  $\text{Mg}^{2+}$ . *A*, current–voltage relations for one patch exposed to 0 ( $\blacktriangle$ ), 5 ( $\bullet$ ), and 10 mM  $[\text{Mg}^{2+}]_i$  ( $\blacksquare$ ). The inset shows the original ensemble averages of the responses to ramp changes of the membrane potential of the excised inside-out patch. *B*, dependence of fractional block on membrane potential. The current in the presence of  $\text{Mg}^{2+}$ , expressed as a fraction of that in its absence ( $i/i_0$ ), is plotted against membrane potential for 5 ( $\bullet$ ) and 10 mM ( $\blacksquare$ )  $[\text{Mg}^{2+}]_i$ . Lines give the results of the fits shown in *C* and *D*. *C*, voltage dependence of  $K_d$ .  $K_d(0)$  is 15.8 mM, and affinity increases e-fold for a 4 mV depolarization.  $\bullet = 5$ ,  $\blacksquare = 10$  mM  $[\text{Mg}^{2+}]_i$ . *D*, concentration dependence of channel blockage. The fit of data shows that the assumption of a Hill coefficient of 1 ( $n = 1$ ) is superior to that assuming a Hill coefficient of 2 ( $n = 2$ ).

The effects of applying  $\text{Mg}^{2+}$  and  $\text{Na}^+$  are shown in Figs 12 and 13 respectively.  $\text{Mg}^{2+}$  was applied at concentrations of 2, 5, and 10 mM;  $\text{Na}^+$  was applied at 10 and 20 mM. The effects on unitary current–voltage relations are shown in Figs 12*A* and 13*A* with the experimental records in the upper left inset. In Figs 12*B* and 13*B*, the ionic blockage is illustrated by showing the current in the absence of a blocking ion ( $i$ ), expressed as a fraction of that in control ( $i_0$ ), plotted against membrane potential. In each case, the fractional block is fitted assuming a single ion binds to block the channel and that:

$$\frac{i}{i_0} = \frac{K_d(V)}{K_d(V) + [C]_i}, \quad (3)$$

where  $[C]_i$  is the concentration of the blocking ion ( $\text{Mg}^{2+}$  or  $\text{Na}^+$ ) and  $K_d(V)$  is the voltage-dependent dissociation constant, whose voltage dependence is given by:

$$K_d(V) = K_d(0) \exp(-z'VF/RT), \quad (4)$$

where  $z'$  is the apparent valency of the blocking ion, that is the real valency  $z$  multiplied by the fraction  $\delta$  of the voltage field working on the ion to bring it to its blocking site (see Figs 12C and 13C).

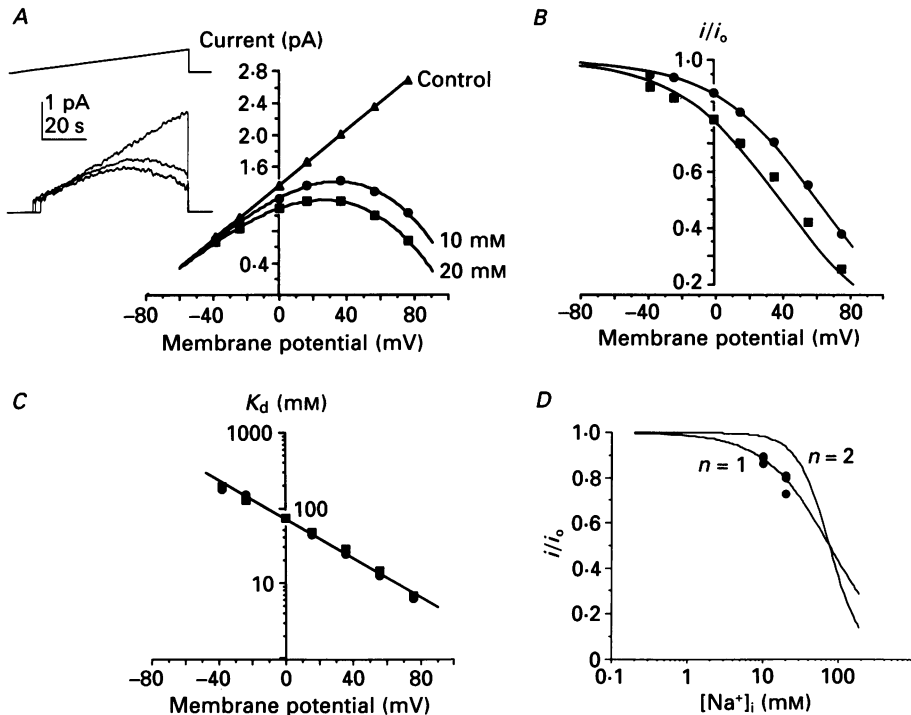


Fig. 13. Voltage-dependence of block by intracellular  $\text{Na}^+$ . *A*, current-voltage relations for one patch exposed to 0 ( $\blacktriangle$ ), 10 ( $\blacksquare$ ), and 20 mM ( $\blacksquare$ )  $[\text{Na}^+]_i$ . The inset shows the original ensemble averages of the responses to ramp changes of the membrane potential of the excised inside-out patch. *B*, dependence of the fractional block on membrane potential. The current in the presence of  $\text{Na}^+$ , expressed as a fraction of that in its absence ( $i/i_0$ ), is plotted against membrane potential for 10 ( $\bullet$ ) and 20 mM ( $\blacksquare$ )  $[\text{Na}^+]_i$ . Lines give the results of the fits shown in *C* and *D*. *C*, voltage dependence of  $K_d$ .  $K_d(0)$  is 68.2 mM, and the affinity increases e-fold for a 32 mV depolarization. *D*, concentration dependence of channel blockage. The fit of data shows that the assumption of a Hill coefficient of 1 ( $n = 1$ ) is superior to that assuming a Hill coefficient of 2 ( $n = 2$ ).

For  $\text{Mg}^{2+}$ ,  $K_d(0)$  was  $15.6 \pm 1.5$  mM ( $n = 6$ ). For  $\text{Na}^+$ ,  $K_d(0)$  was  $76.0 \pm 7.2$  mM ( $n = 3$ ). For  $\text{Mg}^{2+}$ ,  $K_d(V)$  changed e-fold with a 49 mV change in voltage, indicating a value for  $z'$  of 0.51. For  $\text{Na}^+$ ,  $K_d(V)$  changed e-fold with a 32 mV change in voltage, indicating a value for  $z'$  of 0.78. Figures 11D and 12D confirm that block occurs with 1:1 binding of the blocking ion and that attempting to fit the concentration dependence of block assuming a Hill coefficient of 2 gave a poor fit.

In order to confirm that block by intracellular  $\text{Na}^+$  and  $\text{Mg}^{2+}$  can fully account for the rectification, we have compared current-voltage relations for the same channel under on-cell recording and after excision of the patch. After excision the internal surface of the inside-out patch was exposed to an artificial intracellular fluid

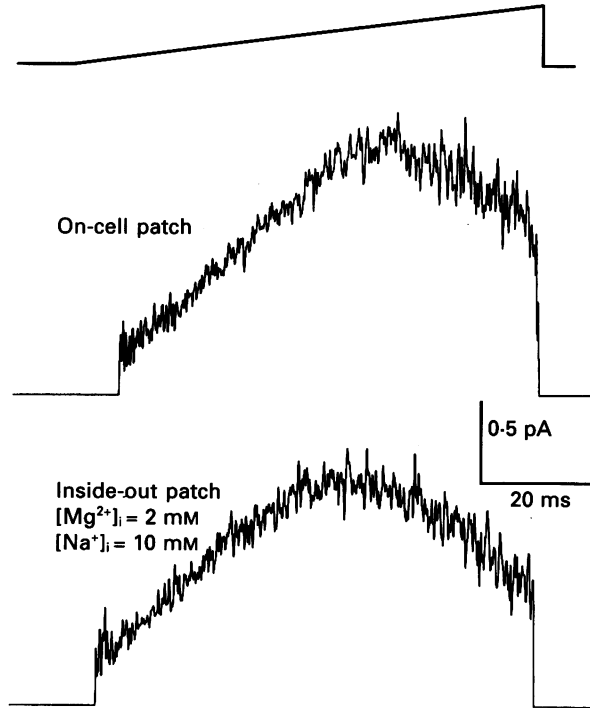


Fig. 14. Blockage by intracellular  $\text{Mg}^{2+}$  and  $\text{Na}^+$  explains the rectification seen during on-cell recording. Unitary A-currents are evoked by stepping the membrane potential from 40 mV negative to the resting potential (on-cell patch) or from  $-100$  mV by 180 mV and then ramping back to the holding potential at  $2.25$  mV  $\text{ms}^{-1}$ . The ionic currents are ensemble averages of currents where one channel was open, formed after subtraction by analog and digital means of the capacity and leakage currents. The solution bathing the cytoplasmic face of the inside-out patch contained  $\text{Mg}^{2+}$  at 2 mM and  $\text{Na}^+$  at 10 mM. The cell resting potential was assumed to be  $-60$  mV in comparing the two results.

containing 10 mM- $\text{Na}^+$  and 2 mM- $\text{Mg}^{2+}$ . The result, shown in Fig. 14, is that the rectification observed on-cell is closely mimicked by these two blocking ions, and such blockage appears sufficient to explain the phenomenon fully. Further, as the inset to Fig. 2 shows the activation of A-current under whole-cell recording may be fitted with the Boltzmann relation used to fit the activation of unitary currents, after modification to take account of channel blockage (see Discussion).

#### *Ionic blockage and channel open time*

In this section, we consider whether the ionic blockage that produces rectification of the channel depends on the state of the channel, for if blocking ions can leave only open channels, measured openings (which are actually bursts of open and blocked states) should become prolonged.

Figure 15 shows the effect of excision of a membrane patch on channel open state probability and on open time. Excision results in the increase in unitary current, already described. As a consequence the ensemble average current also increased, although there is little or no effect on channel open state probability. A consistent

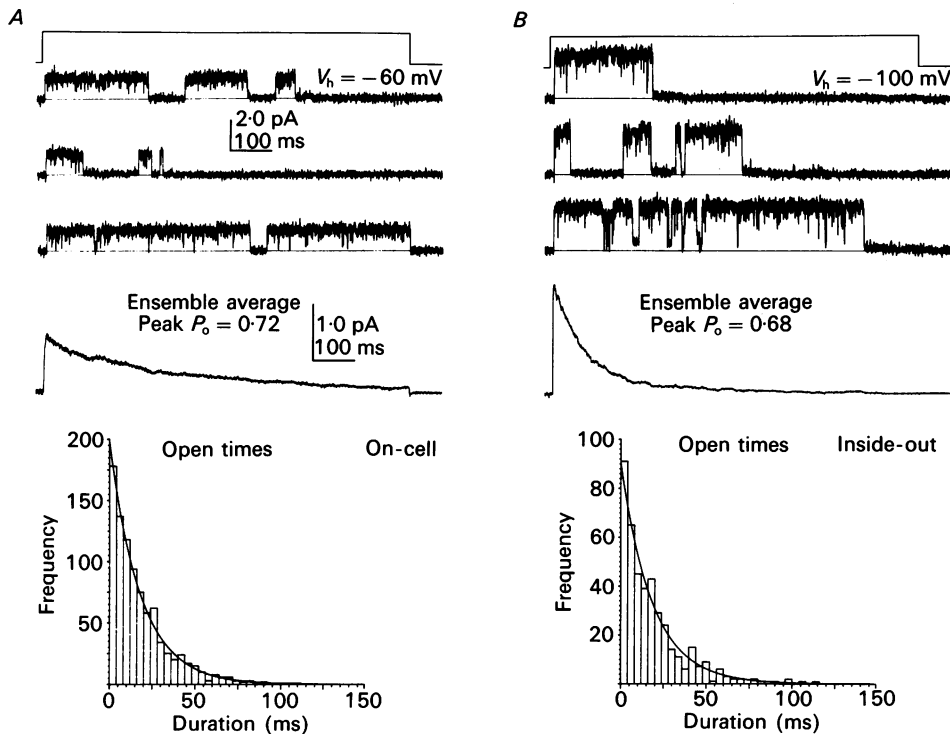


Fig. 15. Patch excision does not affect channel open time. The membrane potential was held 40 mV negative to the resting potential during on-cell recording (*A*) and at  $-100$  mV after patch excision (*B*). In both cases the membrane potential was stepped 100 mV to evoke the currents shown. Unitary current was increased on excision into a solution containing no  $Mg^{2+}$  or  $Na^+$ , but channel  $P_{open}$  was unaffected, being 0.72 during on-cell recording and 0.68 during recording after patch excision. Open time histograms were fitted by a single exponential with  $\tau_{open}$  being 18.2 ms during on-cell recording and 18.5 ms after patch excision.

finding is that inactivation becomes more rapid after patch excision, which contrasts with the finding of Ruppersberg, Stocker, Pongs, Heinemann, Frank & Koenen (1991*b*) that patch excision slows inactivation of channels expressed in oocytes from RCK4. Certainly the speeding of inactivation is not associated with a decrease in channel open time, associated with removal of channel blockage. The mean open time ( $\tau_{open}$ ) was 18.2 ms on cell and 18.5 ms after excision.

Essentially the same result is found when the intracellular surface of an excised patch is exposed to 5 mM- $Mg^{2+}$  (data not shown), though inactivation is not altered in rate by adding  $Mg^{2+}$ .  $\tau_{open}$  was unaltered by the presence or absence of  $Mg^{2+}$  at

5 mM, and was 12.7 ms in the absence and 12.4 ms in the presence of  $\text{Mg}^{2+}$ . Thus  $\text{Mg}^{2+}$  can leave channels when they are either open or closed.

#### DISCUSSION

We have examined the unitary properties of channels which carry A-current in mammalian central neurones, using both cell-attached and excised, inside-out membrane patches. The results indicate a unitary conductance of 17 pS with physiological  $[\text{K}^+]$ . Rectification of the unitary current-voltage relation appears to be due to block by the physiological intracellular cations  $\text{Mg}^{2+}$  and  $\text{Na}^+$ . Preliminary analysis of the kinetic properties indicates a single open state, with several closed states and more than one inactivated state.

##### *Single channel properties*

As described in the Introduction, channels carrying transient outward  $\text{K}^+$  currents are diverse. While the conductance of the A-current channel found in rat locus coeruleus neurones is similar to that previously reported in nodose and dorsal root ganglia (Cooper & Shrier, 1985, 1989; Kasai *et al.* 1986; around 40 pS in symmetrical high  $[\text{K}^+]$  and 17–22 pS with physiological  $[\text{K}^+]_o$  and  $[\text{K}^+]_i$ ), it is higher than that reported for transient outward  $\text{K}^+$  currents of *Drosophila* neurones (6–8 pS; Solc & Aldrich, 1988) and  $\text{GH}_3$  clonal pituitary cells (6–8 pS, Oxford & Wagoner, 1989). More strikingly, it is higher than that for inactivating  $\text{K}^+$  channels expressed in oocytes from the RCK3 or RCK4 sequence from rat brain (9.6 and 4.7 pS respectively; Stühmer *et al.* 1989). There are other notable differences between our own results with native A-current channels and those with channels expressed from the RCK4 clone. We find inactivation increases in rate after patch excision and is not slowed as it is with RCK4 (compare Fig. 15 with the results of Ruppersberg *et al.* 1991*b*). Additionally we do not find channels re-open at negative membrane potentials after inactivation under depolarization (compare Fig. 3 with the results of Ruppersberg, Frank, Pongs & Stocker, 1991*a*).

4-Aminopyridine is known to block A-currents. A relatively slowly inactivating current is blocked by 4-AP in the micromolar concentration range (and is also blocked by dendrotoxin), while a more rapidly inactivating current requires concentrations of 4-AP in the millimolar range (Segal *et al.* 1984; Stanfield *et al.* 1986). A-current in the locus coeruleus inactivates rapidly and is sensitive to millimolar, not micromolar 4-AP. Preliminary experiments on channels carrying A-current in hippocampal neurones grown in tissue culture show them to have identical properties to those described here (Forsythe *et al.* 1990).

##### *Kinetics of channels carrying A-current*

In our analysis of channel kinetics, we have not considered visits to substates separately from full openings. The distributions of open times then indicate a single open state. In addition there are three or four closed states. More than one inactivated state is likely from runs analysis, which, under appropriate conditions, shows clustering of records where the channel fails to open. Because the channel is voltage dependent, the transition towards open from at least one of the closed states

must be voltage dependent. And as expected, the latency to first opening depends strongly on voltage. The dwell time in the open state shows some dependence on voltage, indicating that one or more of the rate constants for leaving the open state is voltage dependent.

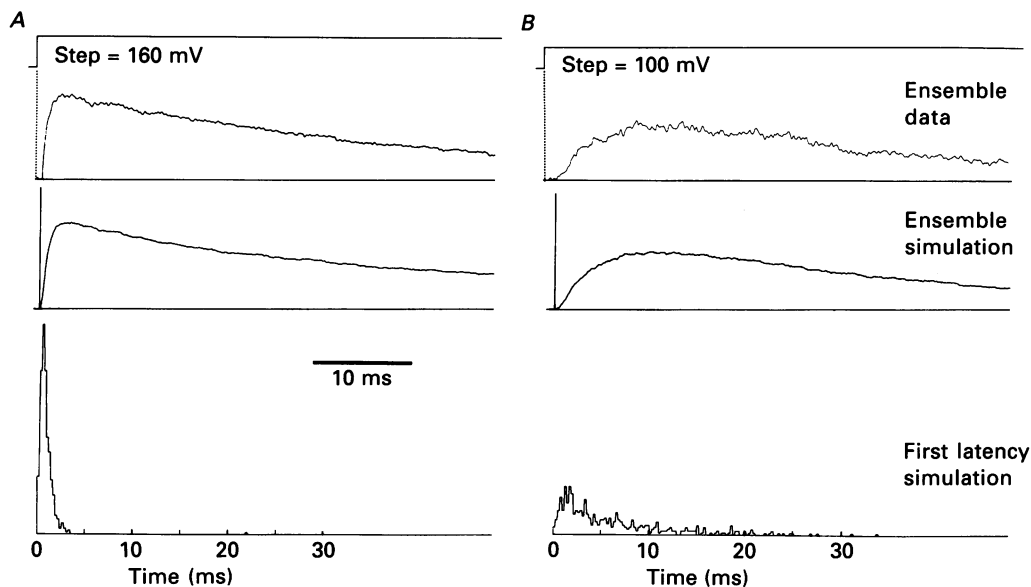
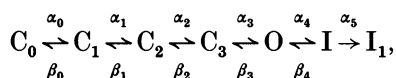


Fig. 16. Simulation of A-channel gating according to the scheme detailed in the text, for step depolarizations to +60 mV (*A*) and 0 mV (*B*) in an excised patch. The top trace is the ensemble average of the respective data for the same patch as described in Fig. 9. The amplitude axis is normalized to 1.0 at +60 mV, so the relative amplitudes reflect the change in open probability (for both the data and simulation traces). The middle trace shows the simulated ensemble average obtained to the proposed kinetic scheme using the following rate constants (ms). In both *A* and *B*:  $\alpha_1$ , 10.0;  $\alpha_2$ , 50.0;  $\alpha_3$ , 3.3;  $\alpha_4$ , 0.045;  $\alpha_5$ , 0.010;  $\beta_0$ , 1.0;  $\beta_1$ , 0.25;  $\beta_2$ , 0.05; and  $\beta_4$ , 0.010. Voltage dependence was ascribed to the rate constants  $\alpha_0$  and  $\beta_3$ . In *A* (+60 mV):  $\alpha_0$ , 2.0 and  $\beta_3$ , 0.025; in *B* (0 mV):  $\alpha_0$ , 0.175 and  $\beta_3$ , 0.087. The lower trace shows the simulated first latencies (see Fig. 9 for measured first latencies). The rise-time, inactivation and relative amplitudes of the ensemble averages and first latency distributions show a reasonable correlation with the simulated values, with the exception that this model does not fully account for the initial delay in channel opening.

Some of these features (though not the substate behaviour) may be explained by a state diagram of the following form:



(see also Solc & Aldrich, 1990), where  $C_0$ ,  $C_1$ ,  $C_2$ , and  $C_3$  are closed states,  $O$  indicates the open state, and  $I$  and  $I_1$  are inactivated states.

In contrast to the neuronal  $A_2$  channel in *Drosophila* (Solc & Aldrich, 1990), the mammalian neuronal A-channel does possess voltage-dependent steps from the open state. It also exhibits multiple populations of closed times during a depolarizing

pulse, implying that the backward rate constants ( $\beta_3$ ,  $\beta_2$ , etc.) are not negligible. The preliminary analysis of bursts for the patch of Fig. 9 shows no substantial voltage dependence for the durations of closures within bursts. Neither was the number of bursts per sweep apparently influenced by voltage. The number of openings per burst did, however, depend on voltage. We now consider a form of the scheme illustrated above where the voltage dependence lies primarily in the first opening step, from  $C_0$  to  $C_1$  (Fig. 16). We consider bursts to occur with the channel returning from open to the closed states  $C_3$ ,  $C_2$ , etc., and, for simplicity and following Solc & Aldrich (1990), consider the intervals between bursts to be associated with visits to the inactivated state I. Channel openings end when the channel enters the absorbing state  $I_1$ .

If we make these assumptions, the number of bursts per trace will be  $(\alpha_5 + \beta_3)/\alpha_5$  if the channel is in one of the closed states (assumed to be  $C_0$  in our calculations) at the start of the depolarizing pulse. The mean number of openings per burst is  $(\alpha_4 + \beta_3)/\alpha_4$ , while the mean open time,  $\tau_{\text{open}}$ , is  $(\alpha_4 + \beta_3)^{-1}$ . These quantities were used to estimate certain of the transition rates in the state diagram;  $\beta_3$  appears to be the voltage dependent transition rate from open.

The state diagram was then modelled using a simulation program written by Dr N. W. Davies (see Davies, Pettit, Agarwal & Standen, 1991). Estimated values of  $\alpha_4$ ,  $\alpha_5$  and  $\beta_3$  (without correction for the limited time resolution of the recording) were used for voltage steps of either 100 or 160 mV and values of the other rate constants adjusted to give the best fit to the ensemble average and first latency distributions. At the start of the voltage pulse, the channel was assumed to be in state  $C_0$ . The values used for the rate constants are given in the legend to Fig. 16. Only one rate constant other than  $\beta_3$  was required to be voltage dependent.

The ensemble averages from the channel of Fig. 9 are shown above each simulation in Fig. 16, with the data normalized to the unitary current amplitude. It can be seen that the time course and relative amplitude of the simulations correspond closely with the results. The model does not, however, account fully for the initial delay in the first latency distribution. The simulation cannot anyway be regarded as a unique solution since the model has a large number of free parameters.

We did not attempt a kinetic analysis of the transitions between fully open and substates partly because we were unable adequately to resolve those to the 0.75 level. A complete kinetic model must clearly explain these transitions.

#### *Rectification of unitary A-current-voltage relations*

The rectification shown by unitary A-current-voltage relations reflects a mechanism common to several  $K^+$  channel types. Rectification of unitary A-current-voltage relations occurs in cells of the nodose ganglion (Cooper & Shrier, 1985), the locus coeruleus (this paper; Linsdell *et al.* 1990), and the hippocampus (Forsythe *et al.* 1990). The phenomenon may not be common to all mammalian A-current channels, since Kasai *et al.* (1986) observed no rectification in channels of neurones of the dorsal root ganglion. However, among other  $K^+$  channels, both inward rectifiers and ATP-dependent  $K^+$  channels show similar block by intracellular cations, specifically  $Mg^{2+}$  and  $Na^+$ . Physiological concentrations of  $Mg^{2+}$  block inward rectifiers (Matsuda, Saigusa & Irisawa, 1987; Vandenburg, 1987), and this block largely accounts for the phenomenon of inward rectification.  $Na^+$  also produces block (Matsuda, 1992). Again in the case of ATP-dependent  $K^+$  channels, both  $Mg^{2+}$

and  $\text{Na}^+$  block. In channels from heart muscle, the two cations may experience a similar fraction of the membrane voltage field, and act with Hill coefficients of 1 and 2 respectively (Horie, Irisawa & Noma, 1987). In skeletal muscle, Hill coefficients are close to one in both cases (Quayle & Stanfield, 1989). In channels carrying A-current, the effective valencies for block are different, and both ions block with a Hill coefficient of one. Further work is in progress to determine the rates of blocking and unblocking by the ions.

The finding that internal cations block A-currents at positive membrane potentials has implications for some of the measurements of potentials at which A-current is half-maximally activated. Thus, the measured inactivation of the whole-cell and of the unitary currents is similar to that reported previously in a variety of neuronal preparations including molluscan neurones (Connor & Stevens, 1971*a*); hippocampal neurones (Numann, Wadman & Wong, 1987); spinal cord neurones (Segal *et al.* 1984); and dorsal root ganglia (Mayer & Sugiyama, 1988). However, the voltage dependence of the activation of the whole-cell currents, estimated in the manner described in the text, did not match that for unitary currents. Further, where estimates have been made of the voltage for half-activation, the values found ( $-33$  mV, Numann *et al.* 1987;  $-33$  mV, Surmeier, Bargas & Kitai, 1988;  $-9$  mV, Mayer & Sugiyama, 1988) are more negative than those found here for single channels.

The discrepancy appears to be a consequence of the strong rectification found in these channels. The effect may be predicted by multiplying the maximum conductance  $G_{\max}$  by the fractions of channels at each voltage left unblocked by  $\text{Mg}^{2+}$  ( $1 - f_{\text{Mg}}$ ) and  $\text{Na}^+$  ( $1 - f_{\text{Na}}$ ). The conductance is then given by:

$$G = \frac{G_{\max}(1 - f_{\text{Mg}})(1 - f_{\text{Na}})}{\{1 + \exp[(V - V')/k]\}}.$$

The modified relation between activation and membrane potential is plotted as the inset to Fig. 2.

### *Physiological significance*

Although the voltage dependence of the block by  $\text{Mg}^{2+}$  and  $\text{Na}^+$  is such that the block is most potent at positive potentials, it is possible that the mechanism could serve a modulatory role. It has been suggested that A-current serves to repolarize the action potential (Belluzzi, Sacchi & Wanke, 1985). Changes in  $[\text{Na}^+]_i$  and  $[\text{Mg}^{2+}]_i$  could therefore modulate the duration of the action potential, and, at nerve terminals,  $\text{Ca}^{2+}$  entry and release of transmitter. Further, by analogy with the mechanism whereby  $\text{Ca}^{2+}$  entry may locally cause activation of  $\text{Ca}^{2+}$ -activated  $\text{K}^+$  channels or inactivation of  $\text{Ca}^{2+}$  channels,  $\text{Na}^+$  entry may also be able to influence A-current locally. One might conjecture that such mechanisms play a role where both  $\text{Na}^{2+}$  and A-current channels are present at high density, perhaps at the axon hillock and initial segment region (see Premack, Thompson & Coombs-Hahn, 1989). In addition, in pathological conditions where  $[\text{Na}^+]_i$  increases (e.g. in epilepsy and excitotoxicity), it is possible that block of A-current will contribute to the feed-forward excitation by reducing the rate of repolarization and decreasing the interval between action potentials.

We are grateful to the Wellcome Trust for support of this work. I. D. F. is a Wellcome Trust Senior Research Fellow in Basic Biomedical Science; P. L. holds an SERC research studentship. We thank Dr Noel Davies for generously allowing us to use his program for simulating ion channel behaviour and Aziza Alibhai and William King for expert technical assistance.

## REFERENCES

- BECKH, S. & PONGS, O. (1990). Members of the RCK potassium channel family are differentially expressed in the rat nervous system. *EMBO Journal* **9**, 777–782.
- BELLUZZI, O., SACCHI, O. & WANKE, E. (1985). A fast transient outward current in the rat sympathetic neurone studied under voltage clamp conditions. *Journal of Physiology* **358**, 91–108.
- BOTTENSTEIN, J. E. & SATO, G. H. (1979). Growth of a neuroblastoma cell line in serum-free supplemented medium. *Proceedings of the National Academy of Sciences of the USA* **74**, 514–517.
- COLQUHOUN, D. (1987). Practical analysis of single channel records. In *Microelectrode Techniques. The Plymouth Workshop Handbook*, ed. Standen, N. B., Gray, P. T. A. & Whitaker, M. J., pp. 83–135. Company of Biologists, Cambridge.
- CONNOR, J. A. & STEVENS, C. F. (1971*a*). Voltage clamp studies of a transient outward membrane current in gastropod neural somata. *Journal of Physiology* **213**, 21–30.
- CONNOR, J. A. & STEVENS, C. F. (1971*b*). Prediction of repetitive firing behaviour from voltage clamp data on an isolated neural soma. *Journal of Physiology* **213**, 31–53.
- COOPER, E. & SHRIER, A. (1985). Single channel analysis of fast transient potassium currents from rat nodose neurones. *Journal of Physiology* **369**, 199–208.
- COOPER, E. & SHRIER, A. (1989). Inactivation of A currents and A channels on rat nodose neurones in culture. *Journal of General Physiology* **94**, 881–910.
- DAVIES, N. W., PETTIT, A. I., AGARWAL, R. & STANDEN, N. B. (1991). The flickery block of ATP-dependent potassium channels of skeletal muscle by internal 4-aminopyridine. *Pflügers Archiv* **419**, 25–31.
- FORSYTHE, I. D. (1991). Microincubator for regulating temperature and superfusion of tissue cultured neurons during electrophysiological or optical studies. In *Methods in Neurosciences*, vol. 4, *Electrophysiology and Microinjection*, ed. Conn, P. M., pp. 301–318. Academic Press Inc., San Diego, CA, USA.
- FORSYTHE, I. D., LINSDELL, P. & STANFIELD, P. R. (1990). Unitary A-channels in central neurones. *Society for Neuroscience Abstracts* **16**, 507.
- FORSYTHE, I. D. & STANFIELD, P. R. (1989). Single channel recording of A-current in neurones from the locus coeruleus, grown in dissociated cell culture. *Journal of Physiology* **417**, 85P.
- FORSYTHE, I. D. & WESTBROOK, G. L. (1988). Slow excitatory postsynaptic currents mediated by N-methyl-D-aspartate receptors on cultured mouse central neurones. *Journal of Physiology* **396**, 515–533.
- FRECH, G. C., VAN DONGEN, A. M. J., SCHUSTER, G., BROWN, A. M. & JOHO, R. H. (1989). A novel potassium channel with delayed rectifier properties isolated from rat brain by expression cloning. *Nature* **340**, 642–645.
- GALVAN, M. (1982). A transient outward current in rat sympathetic neurones. *Neuroscience Letters* **31**, 295–300.
- GIBBONS, J. D. (1971). *Nonparametric Statistical Inference*. McGraw-Hill, New York.
- GUSTAFSSON, B., GALVAN, M., GRAFE, P. & WIGSTROM, H. (1982). A transient outward current in a mammalian central neurone blocked by 4-aminopyridine. *Nature* **299**, 252–254.
- HAGIWARA, S., KUSANO, K. & SAITO, S. (1961). Membrane changes on *Onchidium* nerve cell in potassium rich media. *Journal of Physiology* **155**, 470–489.
- HORIE, M., IRISAWA, H. & NOMA, A. (1987). Voltage-dependent magnesium block of adenosine-triphosphate-sensitive potassium channel in guinea-pig ventricular cells. *Journal of Physiology* **387**, 251–272.
- HORN, R., VANDENBURG, C. A. & LANGE, K. (1984). Statistical analysis of single sodium channels. Effects of N-bromoacetamide. *Biophysical Journal* **45**, 323–335.
- KASAI, H., KAMEYAMA, M., YAMAGUCHI, K. & FUKUDA, J. (1986). Single transient K channels in mammalian sensory neurons. *Biophysical Journal* **49**, 1243–1247.

- LINDELL, P., FORSYTHE, I. D. & STANFIELD, P. R. (1990). Rectification of unitary A-current in cultured rat locus coeruleus neurons is the result of a voltage-dependent block by internal  $Mg^{2+}$  and  $Na^+$ . *Journal of Physiology* **430**, 125P.
- MASUKO, S., NAKAJIMA, Y., NAKAJIMA, S. & YAMAGUCHI, K. (1986). Noradrenergic neurons from the locus coeruleus in dissociated cell culture: culture methods, morphology and electrophysiology. *Journal of Neuroscience* **6**, 3229–3241.
- MATSUDA, H. (1992). Voltage-dependent block by internal sodium ions of the cardiac inwardly rectifying  $K^+$  channel. *Journal of Physiology* **446**, 156P.
- MATSUDA, H., SAIGUSA, A. & IRISAWA, H. (1987). Ohmic conductance through the inwardly rectifying K channel and blocking by internal  $Mg^{2+}$ . *Nature* **325**, 156–159.
- MAYER, M. L. & SUGIYAMA, K. (1988). A modulatory action of divalent cations on transient outward current in culture rat sensory neurones. *Journal of Physiology* **396**, 417–433.
- NUMANN, R. E., WADMAN, W. J. & WONG, R. K. S. (1987). Outward currents of single hippocampal cells obtained from the adult guinea-pig. *Journal of Physiology* **393**, 331–353.
- OXFORD, G. S. & WAGNER, P. K. (1989). The inactivating  $K^+$  current in  $GH_3$  pituitary cells and its modification by chemical reagents. *Journal of Physiology* **410**, 587–612.
- PREMACK, B. A., THOMPSON, S. & COOMBS-HAHN, J. (1989). Clustered distribution and variability in kinetics of transient K channels in molluscan neuron cell bodies. *Journal of Neuroscience* **9**, 4089–4099.
- QUAYLE, J. M. & STANFIELD, P. R. (1989). Block of the ATP-sensitive potassium channel of frog skeletal muscle by internal sodium ions. *Journal of Physiology* **410**, 85P.
- RUPPERSBERG, J. P., FRANK, R., PONGS, O. & STOCKER, M. (1991a). Cloned neuronal  $I_K(A)$  channels reopen during recovery from inactivation. *Nature* **353**, 657–660.
- RUPPERSBERG, J. P., STOCKER, M., PONGS, O., HEINEMANN, S. H., FRANK, R. & KOENEN, M. (1991b). Regulation of fast inactivation of closed mammalian  $I_K(A)$  channels by cysteine oxidation. *Nature* **352**, 711–714.
- SCHWARTZ, T. L., TEMPEL, B. L., PAPAIZIAN, D. M., JAN, Y. N. & JAN, L. Y. (1988). Multiple potassium-channel components are produced by alternative splicing at the *Shaker* locus in *Drosophila*. *Nature* **331**, 137–142.
- SEGAL, M., ROGAWSKI, M. A. & BARKER, J. L. (1984). A transient potassium conductance regulates the excitability of cultured hippocampal and spinal neurons. *Journal of Neuroscience* **4**, 604–609.
- SOLC, C. K. & ALDRICH, R. W. (1988). Voltage-gated potassium channel in larval CNS neurons of *Drosophila*. *Journal of Neuroscience* **8**, 2556–2570.
- SOLC, C. K. & ALDRICH, R. W. (1990). Gating of single non-shaker A-type potassium channels in larval *Drosophila* neurons. *Journal of General Physiology* **96**, 135–165.
- STANDEN, N. B., STANFIELD, P. R. & WARD, T. A. (1985). Properties of single potassium channel in vesicles formed from the sarcolemma of frog skeletal muscle. *Journal of Physiology* **364**, 339–358.
- STANSFELD, C. E., MARSH, S. J., HALLIWELL, J. V. & BROWN, D. A. (1986). 4-Aminopyridine and dendrotoxin induce repetitive firing in rat visceral sensory neurones by blocking a slowly inactivating outward current. *Neuroscience Letters* **64**, 299–304.
- STÜHMER, W., RUPPERSBERG, J. P., SCHRÖTER, K. H., SAKMANN, B., STOCKER, M., GIESE, K. P., PERSCHKE, A., BAUMANN, A. & PONGS, O. (1989). Molecular basis of functional diversity of voltage-gated potassium channels in mammalian brain. *EMBO Journal* **8**, 3235–3244.
- SURMEIER, D. J., BARGAS, J. & KITAI, S. T. (1988). Voltage-clamp analysis of a transient potassium current in rat neostriatal neurons. *Brain Research* **473**, 187–192.
- THOMPSON, S. H. (1977). Three pharmacologically distinct potassium channels in molluscan neurones. *Journal of Physiology* **265**, 465–488.
- TIMPE, L. C., SCHWARZ, T. L., TEMPEL, B. L., PAPAIZIAN, D. M., JAN, Y. N. & JAN, L. Y. (1988). Expression of functional potassium channels from *Shaker* cDNA in *Xenopus* oocytes. *Nature* **331**, 143–145.
- VANDENBURG, C. A. (1987). Inward rectification of a potassium channel in cardiac ventricular cells depends on internal magnesium ions. *Proceedings of the National Academy of Sciences of the USA* **84**, 2560–2564.